Chemistry of *C*-Trimethylsilyl-Substituted Heterocarboranes. 11. Synthetic, Spectroscopic, Structural, and Bonding Studies on the Sodium, Sodium Lithium, and Dilithium Complexed "Carbons Adjacent" *nido*-Carborane Anions $[2\text{-}(SiMe_3)\text{-}3\text{-}(R)\text{-}2,3\text{-}C_2B_4H_{6-n}]^{n-}$ (R = $SiMe_3$, Me, H; *n* = 1, 2). High-Yield Conversion to 1,2-Dicarba-*closo*-hexaborane(6) Derivatives: Precursors to "Carbons Apart" Dianionic Carborane Ligands†

Narayan S. Hosmane,* Anil K. Saxena, Reynaldo D. Barreto, Hongming Zhang, John A. Maguire, Lei Jia, Ying Wang, Aderemi R. Oki, Komel V. Grover, Sarah J. Whitten, Kim Dawson, Michael A. Tolle, Upali Siriwardane, Temesgen Demissie, and Joseph S. Fagner

Department of Chemistry, Southern Methodist University, Dallas, Texas 75275

Received January 28, 1993

The reaction of *nido*-2-$(SiMe_3)$-3-(R)-2,3-$C_2B_4H_6$ with excess NaH in THF or TMEDA produces only the corresponding solvated monosodium *nido* species, 1-Na(THF or TMEDA)-2-$(SiMe_3)$-3-(R)-2,3-$C_2B_4H_5$ [R = $SiMe_3$ (**I** or **X**), Me (**II**), H (**III**)] in almost quantitative yields. Further treatment of this compound in THF or TMEDA with 1 equiv of *t*-BuLi results in the second deprotonation to produce, in 86–94% yields, the corresponding mixed-metal derivative, *closo-exo*-Li(THF or TMEDA)-1-Na(THF or TMEDA)-2-$(SiMe_3)$-3-(R)-2,3-$C_2B_4H_4$ [R = $SiMe_3$ (**IV** or **XI**), Me (**V**), H (**VI**)]. However, the corresponding dilithium derivatives, both the solvated *closo-exo*-4,5-$[(\mu\text{-}H)_2Li(Me_2NCH_2)_2]$-1-Li$[(Me_2NCH_2)_2]$-2,3-$(SiMe_3)_2$-2,3-$C_2B_4H_4$ (**XII**) and unsolvated *closo-exo*-Li-1-Li-2-$(SiMe_3)$-3-(R)-2,3-$C_2B_4H_4$ [R = $SiMe_3$ (**VII**), Me (**VIII**), H (**IX**)] species, were prepared from the reaction of the *nido*-carborane with 2 equiv of *t*-BuLi in TMEDA, THF, and *n*-hexane, respectively. The ^1H, ^7Li, ^{11}B, and ^{13}C NMR spectra and IR spectra of **I**–**XII** are all consistent with their molecular formulas. Molecular weight determinations of **I** and **VII** in benzene solution indicated that the compounds exist as monomers in solution. However, the solid state structures of both **I** and **X**, found by single crystal X-ray analysis, show the complexes to be dimeric in nature. On the other hand, the crystal structure of **XII** supports its monomeric structure in solution. While compound **I** crystallizes in the tricnlinic space group $P\bar{1}$, both **X** and **XII** crystallized in monoclinic space groups $P2_1/n$ and $P2_1/c$ with a = 6.326(17), 11.411(4), and 17.080(4) Å, b = 11.82(4), 12.271(4), and 16.294(4) Å, c = 14.16(5), 17.769(7) and 11.775(4) Å, α = 75.47(25)°, β = 80.58(23), 104.43(3), and 97.73°, γ = 80.50(22)°, V = 1003(5), 2410(1), and 3248(2) Å^3, and Z = 1, 2, and 4, respectively. The final refinements of **I**, **X**, and **XII** converged at R = 0.086, 0.047, and 0.051 and R_w = 0.112, 0.059, and 0.060, respectively. The reactions of $NiCl_2$ with the unsolvated *closo*-dilithiacarboranes (**VII**–**IX**) produced the corresponding *closo*-1-$(SiMe_3)$-2-(R)-1,2-$C_2B_4H_4$ (**XIII**–**XV**) as colorless liquids, thus providing an alternative and inexpensive route for the formation of the "carbons adjacent" 1,2-dicarba-*closo*-hexaborane(6) derivatives.

Introduction

Metallacarboranes, in which metals or metal containing groups are incorporated into electron deficient polyhedral cages, constitute a widely studied class of organometallic compounds that parallel the metallocenes.[1,2] The two most studied carborane ligand systems are those based on the *nido*-$[R_2C_2B_9H_9]^{2-}$ (R = H or a cage carbon substituent) dianions, which yield icosahedral metallacarboranes, and the smaller cage carborane dianions of the type *nido*-$[2,3\text{-}R_2C_2B_4H_4]^{2-}$ (R = H or a cage carbon substituent), that give rise to pentagonal bipyramidal metallacarboranes. The general synthetic routes to these metallacarboranes involve the removal of the acidic B–H–B bridge hydrogens from the neutral *nido*-carboranes and the subsequent coordination of the resulting anions with the desired metal or metal compound. Both mono- and dianions of the larger, C_2B_9, cages can be easily produced by reacting the parent *nido*-$R_2C_2B_9H_{13}$ with bases such as NaH.[3] These anions have been used extensively in the

† Dedicated to Professor John J. Banewicz on the occasion of his retirement from active teaching and research at Southern Methodist University.

(1) Grimes, R. N. In *Comprehensive Organometallic Chemistry*; Wilkinson, G., Stone, F. G. A., Abel, E. W., Eds.; Pergamon: Oxford, U.K., 1982; Vol. 1, Chapter 5.5 (see also references therein).

(2) Hawthorne, M. F.; Young, D. C.; Wegner, P. A. *J. Am. Chem. Soc.* **1965**, *87*, 1818.

(3) Hawthorne, M. F.; Young, D. C.; Andrews, T. D.; Howe, D. V.; Pilling, R. L.; Pitts, A. D.; Reintjes, M.; Warren, L. F.; Wegner, P. A. *J. Am. Chem. Soc.* **1968**, *90*, 879. (b) Wing, R. M. *J. Am. Chem. Soc.* **1970**, *92*, 1187.

0276-7333/93/2312-3001$04.00/0

preparation of a wide variety of metal complexes.[4] On the other hand, dianion formation in the smaller cage system is not so straightforward. In 1966, Onak and Dunks reported the synthesis of the monoanion $[2,3\text{-}C_2B_4H_7]^-$ by the reaction of 2,3-dicarba-*nido*-hexaborane(8) with solid NaH in diglyme.[5] These investigators were unable to prepare the corresponding $[C_2B_4H_6]^{2-}$ dianion even after heating the monoanion with excess NaH at 200 °C.[5] This lack of reactivity of the small cage monoanions is surprising in that, under the usual experimental conditions, the NaH reaction should be irreversible because of the continual removal of the H_2 product. On the other hand, the monoanions react readily with salts such as $SnCl_2$ to form the corresponding neutral metallacarboranes. Structural and spectroscopic studies on the stannacarboranes show that the bridge hydrogens have been removed and that the tin atoms occupy apical positions of the C_2B_4 polyhedra, giving closo structures.[6] Some insight into the selective reactivity of the monoanions was provided in 1989 by our preliminary report[7] on the crystal structure of the monosodium compound *nido*-1-Na(C_4H_8O)-2,3-$(SiMe_3)_2$-2,3-$C_2B_4H_5$ (**I**). The structure showed that the solid consists of an extended array of tightly bound [1-Na(C_4H_8O)-2,3-$(SiMe_3)_2$-2,3-$C_2B_4H_5$]$_2$ dimers that are stacked almost on top of one another. The undeprotonated bridged hydrogens are effectively shielded within the dimeric cluster. If these dimers persist in solution, the bridged hydrogens would be inaccessible to a heterogeneous base such as NaH. The first descriptions of the preparation of $[nido\text{-}(CR)_2B_4H_4]^{2-}$ dianions were those involved in mixed group 1 compounds with the general formula NaLi[2-($SiMe_3$)-3-(R)-2,3-$C_2B_4H_4$] (R = $SiMe_3$, Me, H), prepared *in situ* by reacting the corresponding monosodium derivative with stoichiometric amounts of *n*-BuLi and used without isolation in the syntheses of the group 14 sandwich complexes.[8] These compounds are important not only because they serve as precursors for the facile preparation of a number of heterocarboranes, not easily accessible through the corresponding monosodium derivative,[8] but also because they can be converted to their corresponding "carbons apart" isomers, $[nido\text{-}2\text{-}SiMe_3\text{-}4\text{-}R\text{-}2,4\text{-}C_2B_4H_4]^{2-}$, through a tandem oxidative cage closure, using platinum salts, followed by a reductive cage opening.[9] These isomers have been found to exhibit their own unique organometallic chemistry.[9-12] It is of interest to note that, just as their "carbons adjacent" isomers, the monoanions of the 2,4-dicarbahexaboranes also show a reluctance to further deprotonation.[13]

Although the preparation and spectroscopic characterization of *nido*-carboranes and the sodium lithium and dilithium complexed dianion 2,3-bis(trimethylsilyl)-2,3-dicarba-*nido*-hexaborate(2-) have been detailed, similar characterizations involving other group 1 C_2B_4 carboranes have not been reported.[14] Moreover, with the exception of a monosodium derivative, no crystal structures of any disodium or dilithium complexes have been described. Since preliminary results indicate that steric factors may be as important as bond energies in determining the reactivity of these compounds, further studies of these essentially ionic species are needed. Specifically, it would be of interest to determine if the alkali metals interact directly with the C_2B_3 bonding faces or simply behave as spectator ions with minimal, exo-polyhedral contacts with the cage atoms. We report herein the details of the preparation and characterization of the sodium-complexed monoanion, along with the sodium/lithium and dilithium complexed dianions of the trimethylsilyl-substituted *nido*-carboranes, 2-($SiMe_3$)-3-(R)-2,3-$C_2B_4H_6$ (R = $SiMe_3$, Me, and H), as well as the results of a structural investigation of several monosodium and dilithium complexes of the bis(trimethylsilyl) derivative of this carborane. In addition, we also report an improved synthesis of *closo*-1-($SiMe_3$)-2-(R)-1,2-$C_2B_4H_4$ (R = $SiMe_3$, Me, and H) which avoids the use of expensive platinum reagents.[15]

Experimental Section

Materials. 2,3-Bis(trimethylsilyl)-2,3-dicarba-*nido*-hexaborane(8), 2-(trimethylsilyl)-3-methyl-2,3-dicarba-*nido*-hexaborane(8), and 2-(trimethylsilyl)-2,3-dicarba-*nido*-hexaborane(8) were prepared by the methods of Hosmane et al.[16-19] Prior to use, *N,N,N',N'*-tetramethylethylenediamine, TMEDA (Aldrich), was distilled *in vacuo* and stored over sodium metal. Purity was checked by IR and NMR spectra and boiling point measurements. Benzene, tetrahydrofuran (THF), and *n*-hexane were dried over $LiAlH_4$ and doubly distilled before use. All other solvents were dried over 4-8 mesh molecular sieves (Aldrich) and either saturated with dry argon or degassed before use. Prior to immediate use, NaH (Aldrich) in a mineral oil dipersion was washed repeatedly with dry *n*-pentane. *tert*-Butyllithium, *t*-BuLi (1.7 M solution in pentane obtained from Aldrich), was used as received.

Spectroscopic and Analytical Procedures. Proton, lithium-7, boron-11, and carbon-13 pulse Fourier transform NMR spectra, at 200, 77.7, 64.2, and 50.3 MHz, respectively, were recorded on an IBM-WP200 SY multinuclear NMR spectrometer. Infrared spectra were recorded on a Perkin-Elmer Model 283 infrared spectrophotometer and a Perkin-Elmer Model 1600 FT-IR spectrophotometer. Elemental analyses were obtained from Oneida Research Services (ORS) Inc., Whitesboro, NY. Molecular weights were determined at Galbraith Laboratories, Knoxville, TN.

Synthetic Procedures. All experiments were carried out in Pyrex glass round bottom flasks of 250-mL capacity, containing magnetic stirring bars and fitted with high-

(4) (a) Miller, J. J.; Hawthorne, M. F. *J. Am. Chem. Soc.* **1959**, *81*, 4501. (b) Grafstein, D.; Dvorak, J. *Inorg. Chem.* **1963**, *2*, 1128. (c) Wiesboeck, R. A.; Hawthorne, M. F. *J. Am. Chem. Soc.* **1964**, *86*, 1642. (d) Dunks, G. B.; Wiersema, R. J.; Hawthorne, M. F. *J. Am. Chem. Soc.* **1973**, *95*, 3174. (e) Schubert, D. M.; Manning, M. J.; Hawthorne, M. F. *Phosphorus, Sulphur Silicon Relat. Elem.* **1989**, *41*, 253. (f) Stone, F. G. A. *Adv. Organomet. Chem.* **1990**, *31*, 53.

(5) Onak, T.; Dunks, G. B. *Inorg. Chem.* **1966**, *5*, 439.

(6) (a) Hosmane, N. S.; Sirmokadam, N. N.; Herber, R. H. *Organometallics* **1984**, *3*, 1665. (b) Hosmane, N. S.; de Meester, P.; Maldar, N. N.; Potts, S. B.; Chu, S. S. C.; Heber, R. H. *Organometallics* **1986**, *5*, 772.

(7) Hosmane, N. S.; Siriwardane, U.; Zhang, G.; Zhu, H.; Maguire, J. A. *J. Chem. Soc., Chem. Commun.* **1989**, 1128.

(8) Siriwardane, U.; Islam, M. S.; West, T. A.; Hosmane, N. S.; Maguire, J. A.; Cowley, A. H. *J. Am. Chem. Soc.* **1987**, *109*, 4600.

(9) Hosmane, N. S.; Jia, L.; Zhang, H.; Bausch, J. W.; Prakash, G. K. S.; Williams, R. E.; Onak, T. P. *Inorg. Chem.* **1991**, *30*, 3793.

(10) Grimes, R. N. *Chem. Rev.* **1992**, *92*, 251.

(11) Hosmane, N. S.; Maguire, J. A. *Adv. Organomet. Chem.* **1990**, *30*, 99.

(12) Beck, J. S.; Sneddon, L. G. *Inorg. Chem.* **1990**, *29*, 295.

(13) Abdou, Z. J.; Gomez, F.; Abdou, G.; Onak, T. *Inorg. Chem.* **1988**, *27*, 3679.

(14) Hosmane, N. S.; Barreto, R. D. *Inorg. Synth.* **1992**, *29*, 89.

(15) Hosmane, N. S.; Barreto, R. D.; Tolle, M. A.; Alexander, J. J.; Quintana, W.; Siriwardane, U.; Shore, S. G.; Williams, R. E. *Inorg. Chem.* **1990**, *29*, 2698.

(16) Hosmane, N. S.; Sirmokadam, N. N.; Mollenhauer, M. N. *J. Organomet. Chem.* **1985**, *279*, 359.

(17) Hosmane, N. S.; Mollenhauer, M. N.; Cowley, A. H.; Norman, N. C. *Organometallics* **1985**, *4*, 194.

(18) Hosmane, N. S.; Maldar, N. N.; Potts, S. B.; Rankin, D. W. H.; Robertson, H. E. *Inorg. Chem.* **1986**, *25*, 1561.

(19) Hosmane, N. S.; Islam, M. S.; Burns, E. G. *Inorg. Chem.* **1987**, *26*, 3236.

vacuum Teflon valves. Nonvolatile substances were manipulated in either a drybox or evacuable glovebags under an atmosphere of dry nitrogen. All known compounds among the products were identified by comparing their IR and NMR spectra with those of the authentic samples.

Synthesis of *nido*-1-Na(C_4H_8O)-2-($SiMe_3$)-3-(R)-2,3-$C_2B_4H_5$ [R = $SiMe_3$ (I), Me (II), H (III)]. A tetrahydrofuran (THF) solution (10–15 mL) of *nido*-2,3-($SiMe_3$)$_2$-2,3-$C_2B_4H_6$ (1.34 g, 6.10 mmol), *nido*-2-($SiMe_3$)-3-(Me)-2,3-$C_2B_4H_6$ (1.68 g, 10.40 mmol), or *nido*-2-($SiMe_3$)-3-(H)-2,3-$C_2B_4H_6$ (0.53 g, 3.59 mmol) was poured *in vacuo* onto the heterogeneous mixture of NaH (0.25 g, 10.41 mmol; 0.6 g, 25 mmol; or 0.20 g, 8.33 mmol) and tetrahydrofuran at −78 °C, and the reaction mixture was slowly warmed to room temperature. The flask was occasionally cooled to −196 °C to control the evolution and buildup of H_2 gas. The evolved H_2 gas (quantitative as measured by using a Toepler pump) was pumped out of the flask, and the reaction was allowed to continue further until H_2 evolution ceased. The mixture was then filtered *in vacuo* through a glass frit to collect the filtrate. The solvent from the filtrate was then removed *in vacuo* to collect an off-white solid, 1-Na(C_4H_8O)-2-($SiMe_3$)-3-(R)-2,3-$C_2B_4H_5$. This solid was recrystallized from benzene solution to give transparent needle-shaped crystals [(**I**) 1.87 g, 5.96 mmol, 98%; (**II**) 2.55 g, 9.98 mmol, 96%; (**III**) 0.80 g, 3.31 mol, 92%). Mol wt (in benzene) for **I**: calcd 314 (with one THF) and 241 (THF-free), found 271. Since **I–III** are extremely sensitive to air and/or moisture, reproducible microanalytical data could not be obtained, even for single crystal samples.

Synthesis of *closo-exo*-Li(C_4H_8O)-1-Na(C_4H_8O)-2-($SiMe_3$)-3-(R)-2,3-$C_2B_4H_4$ [R = $SiMe_3$ (IV), Me (V), H (VI)]. A THF solution (15 mL) of the THF-solvated monosodium complex 1-Na(C_4H_8O)-2-($SiMe_3$)-3-(R)-2,3-$C_2B_4H_5$ (R = $SiMe_3$ (**I**), 1.29 g, 4.11 mmol; R = Me (**II**), 1.75 g, 6.85 mmol; R = H (**III**), 0.65 g, 2.69 mmol) was cooled to −78 °C, and to this solution, *t*-BuLi (1.7 M) in pentane (4.08, 6.7, and 2.65 mmol, respectively) was slowly added *in vacuo* with constant stirring. After complete addition of *t*-BuLi, the solution was allowed to warm to room temperature and stirred further for 1 h. The solvents and the volatile *t*-BuH (not measured) in the flask were then removed under vacuum to give an off-white solid which was later recrystallized from benzene to collect transparent and extremely air and moisture sensitive crystals whose reproducible microanalytical data could not be obtained. The yield was nearly quantitative [(**IV**) 1.51 g, 3.85 mmol, 94%; (**V**) 2.13 g, 6.38 mmol, 93%; (**VI**) 0.81 g, 2.53 mmol, 94%].

Synthesis of Unsolvated *closo-exo*-Li-1-Li-2-($SiMe_3$)-3-(R)-2,3-$C_2B_4H_4$ [R = $SiMe_3$ (VII), Me (VIII), H (IX)]. *n*-Hexane solutions (10–15 mL) of *nido*-2,3-($SiMe_3$)$_2$-2,3-$C_2B_4H_6$ (1.204 g, 5.48 mmol), *nido*-2-($SiMe_3$)-3-(Me)-2,3-$C_2B_4H_6$ (1.278 g, 7.91 mmol), and *nido*-2-($SiMe_3$)-3-(H)-2,3-$C_2B_4H_6$ (0.489 g, 3.32 mmol) were cooled to −78 °C, and to each of them was slowly added *in vacuo* *t*-BuLi (1.7 M in pentane) (10.95, 15.85, and 6.67 mmol, respectively) with constant stirring. After complete addition of *t*-BuLi, the mixture was allowed to warm slowly and stirred further for 4 h at room temperature. The solvents and butane (not measured) were pumped out of the reaction flask to collect the corresponding dilithiacarborane as a pale-yellow solid [(**VII**) 1.17 g, 5.05 mmol, 92%; (**VIII**) 1.34 g, 7.73 mmol, 98%; (**IX**) 0.48 g, 3.01 mmol, 91%]. Mol wt (in benzene) for **VII**: calcd 232, found 277. Due to extreme air and moisture sensitivity of **VII–IX** their accurate and reproducible microanalytical data could not be obtained.

The THF-solvated dilithiacarborane [Li(THF)][*closo*-1-Li(THF)-2-($SiMe_3$)-3-(R)-2,3-$C_2B_4H_4$] (R = $SiMe_3$, Me, and H) can be prepared when the above reaction is carried out in THF. However, these species slowly degrade in THF solution and decompose completely after several days with the evolution of H_2 gas to yield lithium borate as one of the products, as identified by ^{11}B and ^7Li NMR spectra.

Synthesis of *nido*-1-Na[(Me_2NCH_2)$_2$]-2,3-($SiMe_3$)$_2$-2,3-$C_2B_4H_5$ (X). A tetramethylethylenediamine (TMEDA) solution (5 mL) of *nido*-2,3-($SiMe_3$)$_2$-2,3-$C_2B_4H_6$ (0.64 g, 2.91 mmol) was poured *in vacuo* onto a heterogeneous mixture of NaH (0.175 g, 7.65 mmol) and TMEDA at −78 °C, and the reaction mixture was slowly warmed to room temperature. The flask was occasionally cooled to −196 °C to control the evolution and buildup of H_2 gas. The evolved H_2 gas was measured (2.92 mmol) and pumped out. The reaction was allowed to continue further until H_2 evolution ceased. The reaction mixture was then filtered *in vacuo* through a glass frit to collect the filtrate. The solvent, TMEDA, was then removed from the filtrate to collect an off-white solid, identified as the TMEDA-solvated *nido*-natracarborane 1-Na[(Me_2NCH_2)$_2$]-2,3-($SiMe_3$)$_2$-2,3-$C_2B_4H_5$ (**X**), in essentially quantitative yield (1.03 g, 2.88 mmol, 99% yield). This solid was recrystallized from hexane solution to give transparent platelike crystals. Anal. Calcd for $C_{14}H_{39}N_2B_4Si_2Na$ (**X**): C, 46.98; H, 10.98; N, 7.82. Found: C, 46.85; H, 11.00; N, 7.35.

Synthesis of *closo-exo*-Li(Me_2NCH_2)$_2$-1-Na[(Me_2NCH_2)$_2$]-2,3-($SiMe_3$)$_2$-2,3-$C_2B_4H_4$] (XI). A 5-mL TMEDA solution of **X** (1.21 g, 3.38 mmol) was cooled to −78 °C, and 3.38 mmol of *t*-BuLi, as a 1.7 M pentane solution, was slowly added *in vacuo* with constant stirring. After complete addition of the *t*-BuLi, the solution was gradually allowed to warm to room temperature and stirred further for 1 h. The solvents and the butane (not measured) in the flask were then removed under high vacuum to collect an off-white solid, identified as **XI**, in 86% yield (1.40 g, 2.92 mmol). The slow recrystallization of **XI** from hexane solution resulted in forming transparent, air sensitive and platelike crystals. The attempts to obtain reproducible microanalytical data for **XI** were unsuccessful.

Synthesis of *closo-exo*-4,5-[(μ-H)$_2$Li(Me_2NCH_2)$_2$]-1-Li[(Me_2NCH_2)$_2$]-2,3-($SiMe_3$)$_2$-2,3-$C_2B_4H_4$ (XII). A TMEDA solution (5 mL) of *nido*-2,3-($SiMe_3$)$_2$-2,3-$C_2B_4H_6$ (1.16 g, 5.28 mmol) was cooled to −78 °C, and to this solution was slowly added *in vacuo* *t*-BuLi (1.7 M in pentane) (10.50 mmol) with constant stirring. When the addition was complete, the mixture was allowed to warm slowly and stirred further for 4 h at room temperature. The solvents and butane (not measured) were then pumped out of the reaction flask to collect the corresponding *closo*-dilithiacarborane **XII** as an off-white solid in 85% yield (2.09 g, 4.5 mmol). A recrystallization of the solid from *n*-hexane solution gave transparent, extremely air and moisture sensitive, platelike crystals whose microanalyses provided irreproducible data.

Synthesis of *closo*-1-($SiMe_3$)-2-(R)-1,2-$C_2B_4H_4$ [(XIII) R = $SiMe_3$; (XIV) R = Me; (XV) R = H]. A 15-mL *n*-hexane solution of the unsolvated *closo*-dilithiacarborane [Li][1-Li-2-($SiMe_3$)-3-(R)-2,3-$C_2B_4H_4$] (R = $SiMe_3$ (**VII**), 3.96 g, 17.11 mmol; R = Me (**VIII**), 4.99 g, 28.8 mmol; R = H (**IX**), 1.13 g, 7.09 mmol) was slowly added to anhydrous $NiCl_2$ (2.22 g, 17.13 mmol; 3.74 g, 28.9 mmol; or 0.92 g, 7.10

Table I. Crystallographic Data[a] for I, X, and XII

	I	X	XII
formula	$C_{24}H_{62}O_2B_8Si_4Na_2$	$C_{28}H_{78}N_4B_8Si_4Na_2$	$C_{20}H_{54}N_4B_4Si_2Li_2$
fw	627.7	715.8	464.0
cryst syst	triclinic	monoclinic	monoclinic
space group	$P\bar{1}$	$P2_1/n$	$P2_1/c$
a, Å	6.326(17)	11.411(4)	17.080(4)
b, Å	11.82(4)	12.271(4)	16.294(4)
c, Å	14.16(5)	17.769(7)	11.775(4)
α, deg	75.47(25)		
β, deg	80.58(23)	104.43(3)	97.73(2)
γ, deg	80.50(22)		
V, Å^3	1003(5)	2410(1)	3248(2)
Z	1	2	4
D_{calcd}, g cm^{-3}	1.04	0.987	0.949
abs coeff, mm^{-1}	0.184	0.159	0.118
crystal dmns, mm	0.42 × 0.15 × 0.32	0.35 × 0.20 × 0.10	0.25 × 0.30 × 0.10
scan type	$\theta/2\theta$	$\theta/2\theta$	$\theta/2\theta$
scan sp in ω; min, max	5.0, 15.0	6.0, 30.0	6.0, 25.0
2θ range, deg	3.0–45.0	3.5–44.0	3.5–42.0
T, K	213	230	230
decay, %	7.0	0	0
no. of data collected	2923	2930	3892
no. of obsd reflctns, $I > 3.0\sigma(I)$	2155	1738	2162
no. of params refined	196	228	305
GOF	3.57	1.76	1.70
g[c]	0.0007	0.0005	0.0005
$\Delta\rho_{(max, min)}$, e/Å^3	+0.58, –0.69	+0.27, –0.24	+0.21, –0.20
R[b]	0.086	0.047	0.051
R_w	0.112	0.059	0.060

[a] Graphite monochromatized Mo Kα radiation, λ = 0.710 73 Å. [b] $R = \sum||F_o| - |F_c||/\sum|F_o|$, $R_w = [\sum w(F_o - F_c)^2/\sum w(F_o)^2]^{1/2}$. [c] $w = 1/[\sigma^2(F_o) + g(F_o)^2]$.

mmol) that was suspended in 5 mL of *n*-hexane at 0 °C. The resulting brown heterogeneous mixture was stirred for 24 h at room temperature. The solvent was then removed at –45 °C under vacuum, leaving behind a dark-brown semisolid residue in the flask which was heated slowly to 115–120 °C to collect a colorless distillate in a detachable U-trap held at –45 °C. This colorless liquid product was later identified as carbons adjacent *closo*-carborane 1,2-$(SiMe_3)_2$-1,2-$C_2B_4H_4$ (**XIII**) (2.20 g, 10.11 mmol, 59%), 1-$(SiMe_3)$-2-(Me)-1,2-$C_2B_4H_4$ (**XIV**) (2.35 g, 14.73 mmol, 51%), or 1-$(SiMe_3)$-2-(H)-1,2-$C_2B_4H_4$ (**XV**) (0.042 g, 0.29 mmol, 4%). No improvement in the yield of **XV** was observed even after the reaction was continued for several days at room temperature. Instead, most of the starting materials were consumed to produce a dark-brown polymeric and insoluble mass which was later discarded. After complete removal of **XIII** or **XIV**, the dark residue in the flask was heated further to 140 °C to collect a small quantity of white solid (in a detachable U-trap at 0 °C) that decomposed in a silica gel column during the purification process and, therefore, could not be identified. The gray-black residue, that remained in the reaction flask after heating at 140 °C, was dissolved in a water/acetone mixture, and the resulting turbid solution was filtered to collect a pale brown filtrate. After removal of all the solvents from the filtrate, a slightly colored solid was obtained (not measured) that was identified as LiCl by qualitative analysis and by comparing its ^{7}Li NMR spectrum with that of the authentic sample. The gray solid, that remained on the frit, was identified by qualitative analysis as elemental nickel (Ni^0). Under the same conditions, the reactions of $NiCl_2$ with the THF- or TMEDA-solvated *closo*-dilithiacarboranes or the corresponding mixed sodium lithium species produced 1.67 g (7.69 mmol, 45% yield) of **XIII** or 1.83 g (11.52 mmol, 40% yield) of **XIV**. However, only a trace quantity of **XV** can be isolated from these reactions.

Crystal Structure Analyses of the Dimeric *nido*-Natracarboranes, 1-Na(C_4H_8O)-2,3-$(SiMe_3)_2$-2,3-$C_2B_4H_5$ (I) and 1-Na$[(Me_2NCH_2)_2]$-2,3-$(SiMe_3)_2$-2,3-$C_2B_4H_5$ (X), and the Zwitterionic *closo*-Dilithiacarborane, *exo*-4,5-$[(\mu$-H$)_2$Li$(Me_2NCH_2)_2]$-1-Li$[(Me_2NCH_2)_2]$-2,3-$(SiMe_3)_2$-2,3-$C_2B_4H_4$ (XII). Colorless, needle-shaped crystals of **I** were grown from a saturated benzene solution, while the colorless, platelike crystals of **X** and **XII** were grown from concentrated *n*-hexane solutions *in vacuo*. Since the crystals change to white amorphous powder upon brief exposure to air and/or moisture, they were sealed with an epoxy resin and mounted rapidly on a Siemens R3m/V diffractometer. The pertinent crystallographic data are summarized in Table I. The final unit cell parameters were obtained by a least-squares fit of 24 accurately centered reflections measured in the ranges $15° < 2\theta < 30°$, $15° < 2\theta < 28°$, and $16° < 2\theta < 30°$ and the intensity data were collected at 230 K in the ranges $3.0° \le 2\theta \le 45.0°$, $3.5° \le 2\theta \le 44.0°$, and $3.5° \le 2\theta \le 42.0°$ for **I**, **X**, and **XII**, respectively. These data were corrected for decay (*ca.* 7%) and absorption in the case of **I** and for Lorentz and polarization effects in all three cases. Three standard reflections monitored after every 150 reflections did not show any significant change in intensity during the data collection. The structures were solved by direct methods using the SHELXTL-Plus package.[20] Full-matrix least-squares refinements were performed and the scattering factors were taken from ref 21. All non-H atoms were refined anisotropically. In the structure of **I**, the cage H atoms H(34), H(3), and H(5) were located, while the positions of H(4) and H(6) were calculated, and all were refined with fixed isotropic thermal parameters. However, the methyl and methylene H atoms were calculated and constrained tetrahedrally. The final cycles of refinement for **I** converged at R = 0.086, R_w = 0.112,

(20) Sheldrick, G. M. *Structure Determination Software Programs*; Siemens X-ray Analytical Instruments Corp.: Madison, WI, 1991.
(21) *International Tables For X-ray Crystallography*; Kynoch Press: Birmingham, U.K., 1974; Vol. IV.

Table II. Atomic Coordinates (×10⁴) and Equivalent Isotropic Displacement Coefficients (Å² × 10³)

	x	y	z	U(eq)[b]		x	y	z	U(eq)[b]
				Compound I					
Na	−2328(3)	5320(2)	3810(1)	40(1)	C(11)	−6003(11)	6889(7)	376(4)	67(3)
Si(1)	−5521(2)	8577(1)	3710(1)	38(1)	C(12)	−2429(9)	7871(6)	957(5)	59(3)
Si(2)	−5353(3)	7670(2)	1261(1)	45(1)	O	−1392(7)	3974(3)	2796(3)	54(2)
C(1)	−5849(7)	7126(4)	3469(3)	29(2)	C(13)	−1533(15)	4232(9)	1780(5)	104(4)
C(2)	−5786(8)	6750(4)	2539(4)	35(2)	C(14)	181(17)	3496(10)	1339(7)	119(5)
B(3)	−6680(10)	5572(6)	2721(5)	37(2)	C(15)	955(22)	2580(8)	2120(7)	141(6)
B(4)	−7546(9)	5206(5)	4001(5)	35(2)	C(16)	−92(14)	2855(6)	3047(5)	77(3)
B(5)	−6793(9)	6257(5)	4379(4)	31(2)	H(34)[a]	−5895(90)	4849(49)	3454(39)	50
B(6)	−8164(9)	6649(5)	3300(4)	32(2)	H(3)[a]	−7145(90)	5212(49)	2208(39)	50
C(7)	−3781(10)	9565(5)	2768(5)	60(3)	H(4)[a]	−8759(90)	4561(48)	4284(39)	50
C(8)	−4201(11)	8246(5)	4843(5)	56(3)	H(5)[a]	−7448(90)	6502(47)	5109(39)	50
C(9)	−8261(9)	9437(5)	3900(5)	59(3)	H(6)[a]	−9644(94)	7172(48)	3154(38)	50
C(10)	−7136(11)	9118(6)	1068(5)	66(3)					
				Compound X					
Na	10849(2)	1293(1)	675(1)	43(1)	C(12)	9500(5)	934(5)	3549(3)	68(2)
Si(1)	7345(1)	2107(1)	439(1)	49(1)	N(21)	11816(4)	3120(3)	631(3)	59(2)
Si(2)	8758(1)	1660(1)	2630(1)	47(1)	N(22)	12744(3)	1329(3)	1802(2)	45(2)
C(1)	8503(4)	1091(3)	946(2)	33(2)	C(23)	12756(6)	3218(5)	1345(4)	90(3)
C(2)	9072(4)	916(3)	1788(2)	35(2)	C(24)	13411(5)	2263(5)	1641(4)	89(3)
B(3)	9714(5)	−189(5)	1918(4)	44(2)	C(25)	10977(7)	3991(6)	620(5)	139(5)
B(4)	9425(5)	−825(5)	995(3)	46(2)	C(26)	12302(8)	3221(6)	−36(4)	145(5)
B(5)	8673(5)	135(5)	433(3)	41(2)	C(27)	12503(6)	1420(6)	2557(3)	95(3)
B(6)	8274(5)	−164(5)	1322(3)	43(2)	C(28)	13488(5)	372(5)	1815(4)	97(3)
C(7)	7303(6)	3447(5)	922(3)	96(3)	H(34)[a]	10335(40)	−393(34)	1395(25)	60(13)
C(8)	5818(4)	1475(5)	229(3)	82(3)	H(3)[a]	10095(38)	−534(35)	2450(25)	58(14)
C(9)	7703(5)	2466(5)	−495(3)	64(2)	H(4)[a]	9630(36)	−1672(38)	899(22)	56(13)
C(10)	9449(5)	3055(4)	2715(3)	66(2)	H(5)[a]	8083(35)	40(32)	−121(23)	43(12)
C(11)	7110(4)	1721(5)	2596(3)	73(3)	H(6)[a]	7455(34)	−462(28)	1415(20)	34(11)
				Compound XII					
Li(1)	2051(4)	10508(5)	3721(7)	44(3)	C(23)	995(4)	11083(5)	5341(6)	118(4)
Li(2)	4365(4)	10875(5)	3348(7)	46(3)	C(24)	844(5)	11615(5)	4434(7)	128(4)
Si(1)	2228(1)	10158(1)	382(1)	49(1)	C(25)	2386(4)	11239(5)	5978(6)	124(4)
Si(2)	1618(1)	8429(1)	2354(1)	48(1)	C(26)	1771(5)	9957(5)	6140(6)	136(4)
C(1)	2440(2)	10067(3)	1965(4)	36(2)	C(27)	1206(4)	11980(4)	2602(6)	112(3)
C(2)	2244(2)	9349(3)	2686(4)	35(2)	C(28)	417(4)	10813(5)	2733(6)	110(4)
B(3)	2787(3)	9328(3)	3862(5)	37(2)	N(31)	5325(2)	10597(2)	2539(3)	38(1)
B(4)	3395(3)	10105(3)	3860(4)	39(2)	N(32)	4941(2)	11936(2)	3941(3)	43(1)
B(5)	3109(3)	10586(3)	2656(5)	39(2)	C(33)	5928(3)	11169(3)	3056(5)	66(2)
B(6)	3220(3)	9490(3)	2582(5)	39(2)	C(34)	5607(3)	11979(3)	3272(5)	75(3)
C(7)	1185(3)	10435(4)	−189(5)	77(2)	C(35)	5608(3)	9753(3)	2694(5)	69(2)
C(8)	2504(3)	9214(3)	−378(5)	86(3)	C(36)	5103(3)	10742(3)	1329(4)	69(2)
C(9)	2814(3)	11008(4)	−143(4)	81(2)	C(37)	4465(4)	12681(3)	3774(5)	87(3)
C(10)	1090(3)	8217(3)	3615(5)	83(3)	C(38)	5227(3)	11848(3)	5152(5)	65(2)
C(11)	817(3)	8506(3)	1118(5)	86(3)	H(3)[a]	2796(20)	8773(23)	4430(31)	39(11)
C(12)	2217(3)	7504(3)	2122(6)	83(3)	H(4)[a]	3952(22)	10166(21)	4435(30)	37(11)
N(21)	1758(3)	10690(4)	5459(4)	79(2)	H(5)[a]	3406(22)	11044(24)	2235(34)	50(12)
N(22)	1044(3)	11309(3)	3327(5)	79(2)	H(6)[a]	3591(22)	9113(22)	2070(32)	41(11)

[a] Cage H atoms were isotropically refined in structures X and XII, while thermal parameters were fixed in structure I. [b] Equivalent isotropic U defined as one-third of the trace of the orthogonalized U_{ij} tensor.

and GOF = 3.57 for 2155 observed refections. Maximum and minimum residuals, 0.58 and −0.69 e/Å³, respectively, were observed in the final difference Fourier maps. The molecule of **X** is a dimer possessing a center of symmetry which is at the midpoint of Na···Na(d) (symmetry operator a: $2 - x, -y, -z$). Carborane cage H atoms were located in DF maps and were isotropically refined. The methyl and methylene H atoms were calculated in the "ride mode" with fixed isotropic temperature factors (U = 0.08 Å²). The final cycles of refinement for **X** converged at R = 0.047, R_w = 0.059, and GOF = 1.76 for 1738 observed refections. Maximum and minimum residuals, +0.27 and −0.24 e/Å³, respectively, were shown in the final difference Fourier maps. Also in the structure of **XII**, the cage H atoms were located in DF maps and were isotropically refined. However, the methyl and methylene H atoms were calculated at idealized positions with fixed isotropic temperature factors (U = 0.08 Å²) and in the ride mode during refinements. The structure of **XII** contains discrete molecules and no significant inter- or intramolecular close contacts have been found. The final cycles of refinement for **XII** converged at R = 0.051, R_w = 0.060, and GOF = 1.70 for 2162 observed refections. Maximum and minimum residuals, +0.21 and −0.20 e/Å³, respectively, were observed in the final DF maps. The final atomic coordinates, including the refined cage H's, are given in Table II, while bond lengths and bond angles are presented in Table III.

Calculations. MNDO–SCF semiempirical molecular orbital calculations were carried out on the model compounds, *closo-exo*-4,5-[(μ-H)₂Li(Me₂NCH₂)₂]-1-Li[(Me₂NCH₂)₂]-2,3-$C_2B_4H_6$ (**XVI**) and {*closo*-1-Li[(Me₂NCH₂)₂]-2,3-$C_2B_4H_6$}⁻ (**XVII**) using version 5.01 of the MOPAC package.[22] The parameters used for lithium, carbon, hydrogen, boron, and nitrogen were those stored in the program. Unless otherwise noted, all geometric parameters were optimized. The starting heavy atom positions for **XVI** were the experimental positions of **XII**, while those of **XVII** were the MNDO optimized positions of the analogous atoms in **XVI**.

(22) Stewart, J. J. P. *QCPE Bull.* **1983**, *3*, 43.

Table III. Selected Bond Lengths (Å) and Bond Angles (deg)[a]

Bond Lengths

Compound I

Na–Cnt(1)[b]	2.778	Na–C(1)	2.832(10)	C(2)–B(6)	1.704(9)	B(3)–B(4)	1.770(10)
Na–C(2)	3.071(11)	Na–B(3)	3.307(11)	B(3)–B(6)	1.747(11)	B(4)–B(5)	1.634(11)
Na–B(4)	3.290(10)	Na–B(5)	2.920(11)	B(4)–B(6)	1.763(10)	B(5)–B(6)	1.802(11)
Na–H(34)	2.57(8)	Na–O	2.346(9)	Si(1)–C(1)	1.880(8)	Si(2)–C(2)	1.867(8)
Na–H(5a)	2.30(6)	Na–B(4a)	2.995(12)	B(3)–H(34)	1.27(6)	B(4)–H(34)	1.26(7)
Na–H(4b)	2.42(7)	Na–B(6b)	3.179(12)	B(3)–H(3)	1.03(8)	B(4)–H(4)	1.13(7)
C(1)–C(2)	1.485(9)	C(1)–B(5)	1.535(8)	B(5)–H(5)	1.13(7)	B(6)–H(6)	1.05(7)
C(1)–B(6)	1.725(10)	C(2)–B(3)	1.536(10)				

Compound X

Na–Cnt(2)	2.774	Na–C(1)	2.846(5)	B(4)–B(5)	1.642(8)	B(4)–B(6)	1.760(9)
Na–C(2)	3.199(5)	Na–B(3)	3.360(7)	B(5)–B(6)	1.787(9)	Si(1)–C(1)	1.875(4)
Na–B(4)	3.191(7)	Na–B(5)	2.799(6)	Si(2)–C(2)	1.862(5)	N(21)–C(23)	1.447(7)
Na–N(21)	2.509(5)	Na–N(22)	2.556(4)	N(21)–C(25)	1.431(9)	N(21)–C(26)	1.434(10)
Na–H(34)	2.58(4)	Na–B(4d)	2.961(7)	N(22)–C(24)	1.444(8)	N(22)–C(27)	1.440(8)
Na–H(5d)	2.39(4)	C(1)–C(2)	1.490(6)	N(22)–C(28)	1.445(7)	C(23)–C(24)	1.419(9)
C(1)–B(5)	1.528(7)	C(1)–B(6)	1.725(7)	B(3)–H(34)	1.32(5)	B(4)–H(34)	1.22(4)
C(2)–B(3)	1.532(7)	C(2)–B(6)	1.702(7)	B(3)–H(3)	1.03(4)	B(4)–H(4)	1.09(5)
B(3)–B(4)	1.770(9)	B(3)–B(6)	1.719(8)	B(5)–H(5)	1.05(4)	B(6)–H(6)	1.05(4)

Compound XII

Li(1)–Cnt(3)	1.906	Li(1)–C(1)	2.367(9)	B(4)–B(6)	1.800(8)	B(5)–B(6)	1.799(8)
Li(1)–C(2)	2.296(9)	Li(1)–B(3)	2.291(9)	Si(1)–C(1)	1.856(5)	Si(2)–C(2)	1.853(4)
Li(1)–B(4)	2.371(9)	Li(1)–B(5)	2.337(10)	N(21)–C(23)	1.441(9)	N(21)–C(25)	1.465(9)
Li(1)–N(21)	2.192(9)	Li(1)–N(22)	2.159(9)	N(21)–C(26)	1.436(10)	N(22)–C(24)	1.477(10)
Li(2)–B(4)	2.226(9)	Li(2)–B(5)	2.241(8)	N(22)–C(27)	1.437(9)	N(22)–C(28)	1.447(8)
Li(2)–H(4)	1.93(4)	Li(2)–H(5)	1.97(4)	C(23)–C(24)	1.372(11)	N(31)–C(33)	1.459(6)
Li(2)–N(31)	2.055(9)	Li(2)–N(32)	2.063(8)	N(31)–C(35)	1.461(6)	N(31)–C(36)	1.443(6)
C(1)–C(2)	1.509(6)	C(1)–B(5)	1.559(6)	N(32)–C(34)	1.470(7)	N(32)–C(37)	1.460(7)
C(1)–B(6)	1.711(6)	C(2)–B(3)	1.560(6)	N(32)–C(38)	1.451(6)	C(33)–C(34)	1.464(8)
C(2)–B(6)	1.702(6)	B(3)–B(4)	1.637(7)	B(3)–H(3)	1.12(4)	B(4)–H(4)	1.10(3)
B(3)–B(6)	1.787(8)	B(4)–B(5)	1.637(7)	B(5)–H(5)	1.06(4)	B(6)–H(6)	1.12(4)

Bond Angles

Compound I

Cnt(1)–Na–O	100.5	Cnt(1)–Na–B(4a)	106.3	Si(2)–C(2)–B(6)	127.3(4)	C(1)–C(2)–B(6)	65.1(4)
Cnt(1)–Na–H(5a)	105	Cnt(1)–Na–H(4b)	176	B(3)–C(2)–B(6)	65.0(4)	C(2)–B(3)–B(4)	104.8(5)
Cnt(1)–Na–B(6b)	129.1	O–Na–B(4a)	127.2(2)	C(2)–B(3)–B(6)	62.1(4)	B(4)–B(3)–B(6)	60.2(4)
O–Na–H(5a)	76(2)	O–Na–H(4b)	83(2)	B(3)–B(4)–B(5)	102.5(5)	B(3)–B(4)–B(6)	59.3(4)
O–Na–B(6b)	100.9(3)	B(4a)–Na–H(4b)	69(2)	B(5)–B(4)–B(6)	63.9(4)	C(1)–B(5)–B(4)	107.7(5)
H(5a)–Na–H(4b)	94.2(3)	B(4a)–Na–B(6b)	96.2(3)	C(1)–B(5)–B(6)	61.6(4)	B(4)–B(5)–B(6)	61.5(4)
B(6b)–Na–H(5a)	124(2)	Na–H(4b)–B(4b)	114(4)	C(1)–B(6)–C(2)	51.3(4)	C(1)–B(6)–B(3)	92.1(4)
Na–H(5a)–B(5a)	104(4)	Si(1)–C(1)–C(2)	131.6(4)	C(2)–B(6)–B(3)	52.8(4)	C(1)–B(6)–B(4)	94.4(4)
Si(1)–C(1)–B(5)	114.0(4)	C(2)–C(1)–B(5)	113.1(5)	C(2)–B(6)–B(4)	98.3(4)	B(3)–B(6)–B(4)	60.5(4)
Si(1)–C(1)–B(6)	128.7(4)	C(2)–C(1)–B(6)	63.6(4)	C(1)–B(6)–B(5)	51.6(4)	C(2)–B(6)–B(5)	91.9(4)
B(5)–C(1)–B(6)	66.8(4)	Si(2)–C(2)–C(1)	127.1(4)	B(3)–B(6)–B(5)	96.9(4)	B(4)–B(6)–B(5)	54.6(4)
Si(2)–C(2)–B(3)	119.7(5)	C(1)–C(2)–B(3)	111.7(5)	Na–O–C(13)	125.7(5)	Na–O–C(16)	124.6(4)

Compound X

Cnt(2)–Na–N(21)	142.8	Cnt(2)–Na–N(22)	106.5	B(5)–B(4)–B(6)	63.3(4)	C(1)–B(5)–B(4)	108.2(4)
Cnt(2)–Na–B(4d)	110.6	Cnt(2)–Na–H(5d)	108	C(1)–B(5)–B(6)	62.1(3)	B(4)–B(5)–B(6)	61.6(4)
N(21)–Na–N(22)	73.5(1)	N(21)–Na–B(4d)	94.6(2)	C(1)–B(6)–C(2)	51.5(3)	C(1)–B(6)–B(3)	92.3(4)
N(22)–Na–B(4d)	130.2(2)	N(21)–Na–H(5d)	109(1)	C(2)–B(6)–B(3)	53.2(3)	C(1)–B(6)–B(4)	95.0(4)
N(22)–Na–H(5d)	85(1)	B(4d)–Na–H(5d)	53(1)	C(2)–B(6)–B(4)	99.6(4)	B(3)–B(6)–B(4)	61.2(3)
Na–H(5d)–B(5d)	101(2)	Si(1)–C(1)–C(2)	131.0(3)	C(1)–B(6)–B(5)	51.5(3)	C(2)–B(6)–B(5)	92.7(4)
Si(1)–C(1)–B(5)	113.7(3)	C(2)–C(1)–B(5)	113.6(4)	B(3)–B(6)–B(5)	97.6(4)	B(4)–B(6)–B(5)	55.1(3)
Si(1)–C(1)–B(6)	128.5(3)	C(2)–C(1)–B(6)	63.5(3)	Na–N(21)–C(23)	106.5(3)	Na–N(21)–C(25)	111.7(4)
B(5)–C(1)–B(6)	66.3(3)	Si(2)–C(2)–C(1)	127.8(3)	C(23)–N(21)–C(25)	107.3(5)	Na–N(21)–C(26)	111.5(4)
Si(2)–C(2)–B(3)	119.6(3)	C(1)–C(2)–B(3)	110.6(4)	C(23)–N(21)–C(26)	111.2(5)	C(25)–N(21)–C(26)	108.6(6)
Si(2)–C(2)–B(6)	125.9(3)	C(1)–C(2)–B(6)	65.0(3)	Na–N(22)–C(24)	104.1(3)	Na–N(22)–C(27)	114.2(3)
B(3)–C(2)–B(6)	64.0(3)	C(2)–B(3)–B(4)	106.2(4)	C(24)–N(22)–C(27)	110.8(5)	Na–N(22)–C(28)	112.2(3)
C(2)–B(3)–B(6)	62.8(3)	B(4)–B(3)–B(6)	60.6(3)	C(24)–N(22)–C(28)	108.2(4)	C(27)–N(22)–C(28)	107.3(4)
B(3)–B(4)–B(5)	101.3(4)	B(3)–B(4)–B(6)	58.3(3)	N(21)–C(23)–C(24)	117.6(5)	N(22)–C(24)–C(23)	118.4(5)

Compound XII

Cnt(3)–Li(1)–N(21)	137.2	Cnt(3)–Li(1)–N(22)	141.7	C(2)–B(6)–B(4)	93.9(3)	B(3)–B(6)–B(4)	54.3(3)
N(21)–Li(1)–N(22)	81.0(3)	N(31)–Li(2)–N(32)	88.1(3)	C(1)–B(6)–B(5)	52.7(3)	C(2)–B(6)–B(5)	91.1(3)
N(31)–Li(2)–H(4)	124(1)	N(31)–Li(2)–H(5)	111(1)	B(3)–B(6)–B(5)	92.7(4)	B(4)–B(6)–B(5)	54.1(3)
N(32)–Li(2)–H(4)	117(1)	N(32)–Li(2)–H(5)	115(1)	Li(1)–N(21)–C(23)	106.6(4)	Li(1)–N(21)–C(25)	103.0(4)
H(4)–Li(2)–H(5)	100(2)	Li(2)–H(4)–B(4)	91(2)	C(23)–N(21)–C(25)	111.8(6)	Li(1)–N(21)–C(26)	114.8(5)
Li(2)–H(5)–B(5)	90(2)	Si(1)–C(1)–C(2)	126.8(3)	C(23)–N(21)–C(26)	111.7(6)	C(25)–N(21)–C(26)	108.6(5)
Si(1)–C(1)–B(5)	120.7(3)	C(2)–C(1)–B(5)	109.2(4)	Li(1)–N(22)–C(24)	106.7(4)	Li(1)–N(22)–C(27)	112.1(5)
Si(1)–C(1)–B(6)	120.4(3)	C(2)–C(1)–B(6)	63.5(3)	C(24)–N(22)–C(27)	110.7(5)	Li(1)–N(22)–C(28)	106.4(4)
B(5)–C(1)–B(6)	66.6(3)	Si(2)–C(2)–C(1)	132.4(3)	C(24)–N(22)–C(28)	111.7(6)	C(27)–N(22)–C(28)	109.1(5)
Si(2)–C(2)–B(3)	115.2(3)	C(1)–C(2)–B(3)	111.6(3)	N(21)–C(23)–C(24)	115.4(6)	N(22)–C(24)–C(23)	115.5(7)
Si(2)–C(2)–B(6)	129.5(3)	C(1)–C(2)–B(6)	64.1(3)	Li(2)–N(31)–C(33)	103.2(4)	Li(2)–N(31)–C(35)	114.9(4)
B(3)–C(2)–B(6)	66.2(3)	C(2)–B(3)–B(4)	106.4(4)	C(33)–N(31)–C(35)	110.2(4)	Li(2)–N(31)–C(36)	107.5(3)
C(2)–B(3)–B(6)	60.7(3)	B(4)–B(3)–B(6)	63.3(3)	C(33)–N(31)–C(36)	112.6(4)	C(35)–N(31)–C(36)	108.4(4)
B(3)–B(4)–B(5)	104.8(4)	B(3)–B(4)–B(6)	62.4(3)	Li(2)–N(32)–C(34)	103.2(4)	Li(2)–N(32)–C(37)	114.8(4)
B(5)–B(4)–B(6)	62.9(3)	C(1)–B(5)–B(4)	107.8(4)	C(34)–N(32)–C(37)	110.2(4)	Li(2)–N(32)–C(38)	109.4(4)
C(1)–B(5)–B(6)	60.8(3)	B(4)–B(5)–B(6)	63.0(3)	C(34)–N(32)–C(38)	110.4(4)	C(37)–N(32)–C(38)	108.8(4)
C(1)–B(6)–C(2)	52.5(2)	C(1)–B(6)–B(3)	93.0(3)	N(31)–C(33)–C(34)	112.9(4)	N(32)–C(34)–C(33)	112.5(5)
C(2)–B(6)–B(3)	53.0(3)	C(1)–B(6)–B(4)	94.7(3)				

[a] Symmetry operator, in structure I: (a) $-1-x, 1-y, 1-z$; (b) $1+x, y, z$. In structure X: (a) $2-x, -y, -z$. [b] Cnt(1), Cnt(2), and Cnt(3) are the centroids of the C2B3 rings in structures I, X, and XII, respectively.

Scheme I

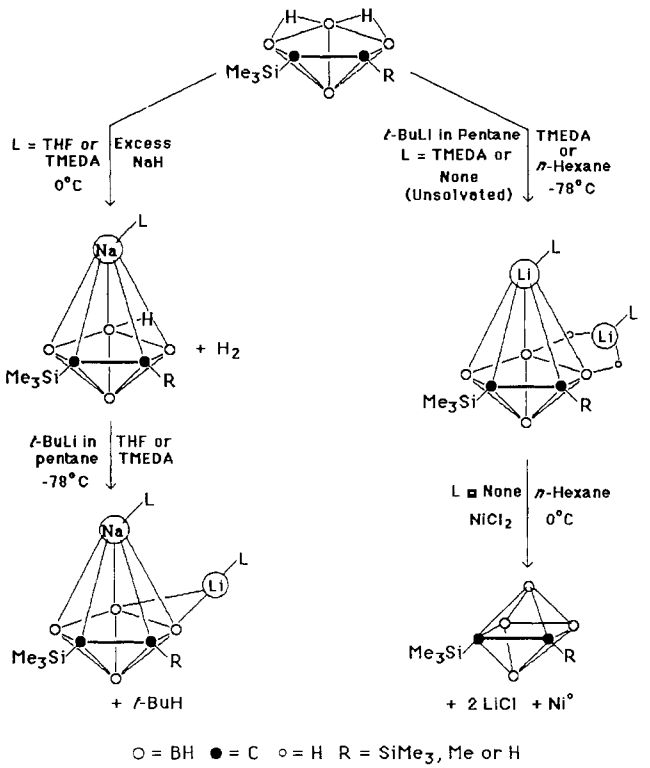

Results and Discussion

Synthesis. The reaction of *nido*-2-($SiMe_3$)-3-(R)-2,3-$C_2B_4H_6$ with excess NaH in either THF or TMEDA produced the corresponding solvated monosodium nido species, 1-Na(THF or TMEDA)-2-($SiMe_3$)-3-(R)-2,3-$C_2B_4H_5$ [R = $SiMe_3$ (**I** or **X**), Me (**II**), H (**III**)] in almost quantitative yields. Although NaH was always present in at least a 2:1 molar ratio, no evidence was found for a further reaction of the carboranes with NaH beyond the 1:1 stoichiometry. This is consistent with earlier results on the unsubstituted carboranes.[5,23] However, further treatment of the monoanions with 1 equiv of *t*-BuLi, in THF or TMEDA, resulted in the quantitative removal of the second bridged proton to produce, in 86–94% yields, the corresponding mixed-metal derivatives, *closo-exo*-Li(THF or TMEDA)-1-Na(THF or TMEDA)-2-($SiMe_3$)-3-(R)-2,3-$C_2B_4H_4$ [R = $SiMe_3$ (**IV** or **XI**), Me (**V**), H (**VI**)]. On the other hand, the corresponding solvated and unsolvated dilithium compounds, *closo-exo*-4,5-[(μ-H)$_2$Li(Me_2NCH_2)$_2$]-1-Li[(Me_2NCH_2)$_2$]-2,3-($SiMe_3$)$_2$-2,3-$C_2B_4H_4$ (**XII**) and *closo-exo*-Li-1-Li-2-($SiMe_3$)-3-(R)-2,3-$C_2B_4H_4$ [R = $SiMe_3$ (**VII**), Me (**VIII**), H (**IX**)], could be prepared by the reaction of the corresponding *nido*-carboranes with 2 equiv of *t*-BuLi in TMEDA, THF, and *n*-hexane, respectively, as shown in Scheme I. The extreme air and/or moisture sensitivity of the compounds made it difficult to obtain reproducible microanalytical data. Compound **X** was the only compound for which reliable analytical data could be obtained; the analytical results are quite consistent with the formula *nido*-1-Na[(Me_2NCH_2)$_2$]-2,3-($SiMe_3$)$_2$-2,3-$C_2B_4H_5$, which was further confirmed by X-ray crystallography. Therefore, the formulations for the compounds **II**–**IX** and **XI**, given in the Experimental Section, are based on their spectroscopic similarities to those that have been structurally characterized (**I**, **X**, and **XII**) and on their similar synthetic routes.

(23) Savory, C. G.; Wallbridge, M. G. H. *J. Chem. Soc., Dalton Trans.* **1974**, 880.

The synthetic utility of the mixed-metal derivatives, **IV**–**VI**, has already been demonstrated in the preparation of a number of metallacarboranes of main-group and early transition elements.[8,11,24,25] Their preparation involves the reaction of the particular sodium/lithium carborane with a metal halide salt, to give the metallacarborane and the group 1 halide. When $NiCl_2$ was chosen as the metal reagent for the reaction of the unsolvated *closo*-dilithiacarboranes (**VII**–**IX**), the THF- or TMEDA-solvated dilithium derivatives (**XII**), or the mixed sodium lithium compounds (**IV**–**VI**, **XI**), a colorless liquid, identified as *closo*-1-($SiMe_3$)-2-(R)-1,2-$C_2B_4H_4$, was produced as the major volatile carborane containing product in 51 to 59% yields, along with a small quantity of an unidentified white solid byproduct, when R = $SiMe_3$ or Me (see Scheme I). However, the reaction of **IX** (R = H) with $NiCl_2$ produced the corresponding *closo*-carborane in very poor yields of 4%; most of the carborane ended up in a dark-brown polymeric mass. The reason for this reactivity difference is not known. Perhaps, the acidic nature of the hydrogen atom on the cage carbon is responsible for some side reaction with the nickel reagent that promotes, or causes, decomposition to the polymer. With this exception, the present reactivity study of the dilithium species produces a new and an inexpensive route for the formation of the carbons adjacent 1,2-dicarba-*closo*-hexaborane(6) derivatives. Prior to these results the most direct route to the *closo*-carboranes involved the initial preparation of *closo*-stannacarborane precursors, followed by their oxidative cage closure using expensive platinum reagents.[15] These *closo*-C_2B_4 carboranes can be reductively opened, in essentially quantitative reactions, to generate the corresponding *nido*-carborane dianions in which the cage carbons in the open C_2B_3 faces are separated by a boron atom (the carbons apart isomers).[9] Since these dianions can act as ligands for a variety of metals,[26] an efficient, inexpensive synthetic method for preparing the 1,2-dicarba-*closo*-hexaborane(6) compounds, **XIII** and **XIV**, is an important development in the extension of the study of the chemistry of carboranes and metallacarboranes.

Spectra. Compounds **I**–**XV** were all characterized by ^1H, ^{11}B, and ^{13}C pulse Fourier transform NMR (Table IV) and IR (Table V) spectroscopy. The ^7Li NMR spectra were obtained for **V** and **XII**.

The ^1H NMR spectra of **III**, **IV**, and **VIII** are shown in Figure 1 and are representative of the monosodium, sodium lithium, and dilithium compounds, respectively. All show sharp resonances due to $SiMe_3$ protons between +0.52 and −0.01 ppm, as well as resonances due to the metal-bound THF or TMEDA molecules. The ^1H NMR spectrum of the monosodium species (**I**–**III**, **X**) shows a broad signal around −5 ppm, corresponding to B–H–B hydrogen. These are shifted downfield somewhat from those of the bridged protons in the respective neutral *nido*-carboranes.[16] The disappearance of the B–H–B resonances in the sodium lithium and dilithium compounds is evidence of the second deprotonation to form the C_2B_4 carborane dianions. All compounds show peaks in the +2 to +5 ppm region due to the basal B–H hydrogens. The apical BH

(24) Oki, A. R.; Zhang, H.; Maguire, J. A.; Hosmane, N. S.; Ro, H.; Hatfield, W. E. *Organometallics* **1991**, *10*, 2996. Oki, A. R.; Zhang, H.; Maguire, J. A.; Hosmane, N. S.; Ro, H.; Hatfield, W. E.; Moscherosch, M.; Kaim, W. *Organometallics* **1992**, *11*, 4202.

(25) (a) Siriwardane, U.; Zhang, H.; Hosmane, N. S. *J. Am. Chem. Soc.* **1990**, *112*, 9637. (b) Oki, A. R.; Zhang, H.; Hosmane, N. S.; Ro, H.; Hatfield, W. E. *J. Am. Chem. Soc.* **1991**, *113*, 8531.

(26) Zhang, H.; Wang, Y.; Saxena, A. K.; Oki, A. R.; Maguire, J. A.; Hosmane, N. S. *Organometallics*, in press.

Table IV. FT NMR Spectral Data[a]

compd	δ, splitting, assignt [$^1J(^{11}B-^1H)$ or $^1J(^{13}C-^1H)$, Hz]	rel area
	200.13-MHz ^1H NMR Data[b]	
I	4.05, q (vbr), basal H (140); 3.52, s (br), THF; 3.17, q (vbr), basal H (138); 1.44, s (br), THF; 0.52, s, Me_3Si; –0.69, q (br), apical H (173); –4.37, s (br), bridge H	2:4:1:4:18:1:1
II	3.58, s, THF; 3.18, q (vbr), basal H [$^1J(^{11}B-^1H)$ = unresolved]; 1.78, s, THF; 2.07, s, Me; 0.13, s, Me_3Si; –0.255, q, apical H (147); –4.98, s (br), bridge H	4:3:4:3:9:1:1
III	6.54, s, CH; 3.54, q (br), basal H (122); 3.48, s (br), THF; 1.69, s (br), THF; 0.01, s, Me_3Si; –2.08, q (br), apical H (161); –5.03, s (br), bridge H	1:3:4:4:9:1:1
IV	3.65, s, THF; 3.38, q (br), basal H [$^1J(^{11}B-^1H)$ = unresolved]; 1.79, s, THF; 0.14, s, $SiMe_3$; –2.02, q (br), apical H (151)	8:3:8:18:1
V	4.05, q (br), basal H [$^1J(^{11}B-^1H)$ = unresolved]; 3.61, s, THF; 1.98, s, Me; 1.58, s, THF; 0.36, s, Me_3Si; –1.83, q, apical H (156)	3:8:3:8:9:1
VI	6.56, s, CH; 3.84, q, basal H (124); 3.62, s (br), THF; 1.70, s (br), THF; 0.23, s, Me_3Si	1:3:8:8:9
VII	3.68, q (br), basal H (119); 0.14, s, $SiMe_3$; –2.0 q (br), apical H (160)	3:18:1
VIII	3.25, q (br), basal H (120); 2.0, s, Me; 0.00, s, $SiMe_3$; –1.93, q (vbr), apical H (142)	3:3:9:1
IX	6.75, s, CH; 3.21, q (br), basal H (148); 0.24, s, Me_3Si; –3.96, br, apical H (unresolved)	1:3:9:1
X	2.18, s, CH_2; 2.03, s, Me; 0.54, s, $SiMe_3$; –2.06, q (br), apical H (unresolved); –4.37, s (br), bridge H	4:12:18:1:1
XI	2.29, s, CH_2; 2.08, s, Me; 0.10, s, $SiMe_3$; –2.00, q (br), apical H (unresolved)	4:12:18:1
XII	4.23, q (br), basal H; 2.35, s, CH_2; 2.06, s, Me; 0.59, s, Me_3Si	3:4:12:18
XIII	1.79, q (br), basal H (160); 0.65, q (br), apical H (179); –0.89, s, $SiMe_3$	1:1:9
XIV	3.22, q (br), basal H (163); 1.74, s, Me; 0.17, s, Me_3Si; –0.45, q (br), apical H (180)	2:3:9:2
XV	6.72, s (br), CH; 2.83, basal H (unresolved); 0.10, s, Me_3Si; 0.83, q (br), apical H (unresolved)	1:2:9:2
	64.21-MHz ^{11}B NMR Data[c]	
I	14.08, d (vbr), basal BH (141); –3.78, d (vbr), basal BH (140); –50.76, d, apical BH (175)	2:1:1
II	19.88, d (br), basal BH (103); 10.97, d (vbr), basal BH (120); 1.93, d, basal BH (107); –44.08, d (br), apical BH (159)	1:1:1:1
III	14.15, d, basal BH (130); 6.88, d (br), basal BH (127); –2.86, d, basal BH (131); –52.48, d (br), apical BH (160)	1:1:1:1
IV	20.85, d (br), basal BH (112); 2.39, d (br), basal BH (88); –44.53, d (br), apical BH (161)	2:1:1
V	16.07, d, basal BH (153); 6.40, d (br), basal BH (133); –2.09, d, basal BH (136); –48.16, d (br), apical BH (157)	1:1:1:1
VI	19.13, d, basal BH [$^1J(^{11}B-^1H)$ = unresolved]; 11.36, d (br), basal BH (131); 1.92, d, basal BH (109); –47.74, d (br), apical BH (161)	1:1:1:1
VII	20.94, d (br), basal BH (119); 2.36, d, basal BH [$^1J(^{11}B-^1H)$ = unresolved]; –44.50, d, apical BH (159)	2:1:1
VIII	20.87, d, basal BH [$^1J(^{11}B-^1H)$ = unresolved]; 10.80, d, basal BH (130); 2.53, d (br), basal BH [$^1J(^{11}B-^1H)$ = unresolved]; –44.66, d, apical BH (157)	1:1:1:1
IX	10.27, d, basal BH [$^1J(^{11}B-^1H)$ = unresolved]; 0.16, d (v br), basal BH [$^1J(^{11}B-^1H)$ = unresolved]; –47.72, d (br), apical BH (128)	1:2:1
X	15.68, d (vbr), basal BH [$^1J(^{11}B-^1H)$ = unresolved]; 1.92, d, basal BH (155.9); –49.73, d, apical BH (165)	2:1:1
XI	19.98, d (br), basal BH [$^1J(^{11}B-^1H)$ = unresolved]; 1.39, d (br), basal BH [$^1J(^{11}B-^1H)$ = unresolved]; –45.28, d (br), apical BH (154)	2:1:1
XII	18.16, d, basal BH [$^1J(^{11}B-^1H)$ = unresolved]; 3.18, d, basal BH [$^1J(^{11}B-^1H)$ = unresolved]; –48.40, d, apical BH [$^1J(^{11}B-^1H)$ = unresolved]	2:1:1
XIII	9.98, d, BH (159.5); –9.85, d, BH (179.5)	1:1
XIV	8.50, d, BH (158); –2.57, d, BH (165); –10.95, d, BH (183)	1:1:2
XV	6.50, d, BH (unresolved); 2.80, d, BH (175); –12.78, d, BH (182)	1:1:2
	50.32-MHz ^{13}C NMR Data[b,d]	
I	113.60, s (br), cage C(SiCB); 68.03, t, THF (145.8); 25.82, t, THF (132.80); 1.99, q, Me_3Si (118)	1:1:1:3
II	124.39, s, cage C(SiCB); 99.21, s, cage CMe; 23.19, q, Me (124); 1.79, q, Me_3Si (118)	1:1:1:3
III	108.59, s, cage C(SiCB); 98.93, d, cage CH (148); –0.32, q, Me_3Si (118)	1:1:3
IV	109.32, s, cage C(SiCB); 3.46, q, Me_3Si (118)	1:3
V	125.55, s, cage C(SiCB); 103.76, s, cage CMe; 21.86, q, Me (125); 1.46, q, Me_3Si (118)	1:1:1:3
VI	124.93, s, cage C(SiCB); 97.5, d, cage CH (138); 0.44, q, Me_3Si (118)	1:1:3
VII	98.88, s, cage C(SiCB); 3.51, q, Me_3Si (118)	1:3
VIII	115.18, s, cage C(SiCB); 108.84, s, cage CMe; 21.12, q, Me (130); 1.26, q, Me_3Si (119)	1:1:1:3
IX	127.51, s, cage C(SiCB); 108.09, d, cage CH (136); 1.00, q, Me_3Si (119)	1:1:3
X	110.91, s, cage C(SiCB); 57.57, t, CH_2 (132.6); 46.34, q, Me (133.15); 3.60, q, Me_3Si (118.5)	1:1:2:3
XI	106.2, s, cage C(SiCB); 56.02, t, CH_2 (133.3); 45.31, q, Me (134.8); 3.60, q, Me_3Si (118.4)	1:1:2:3
XII	97.81, s, cage C(SiCB); 56.60, t, CH_2 (134.3); 45.81, q, Me (134.2); 4.60, q, Me_3Si (118.1)	1:1:2:3
XIII	68.93, s, cage C(SiCB); –0.05, q, Me_3Si (119.9)	1:3
XIV	69.1, s, cage C(SiCB); 67.42, s, cage CMe; 12.47, q, Me (143); –0.69, q, Me_3Si (122)	1:1:1:3
XV	64.35, s (br), cage C(SiCB); 55.63, d, cage CH (178); –2.00, q, Me_3Si (120)	1:1:3
	77.7-MHz ^7Li NMR Data[d,e]	
V	–1.82, s (br), *exo*-cage Li	
XII	–1.60, s (v br), *exo*-cage Li; –6.08, s (v br), *endo*-cage Li	~1:1

[a] C_6D_6 was used as solvent and an internal standard of δ = 7.15 ppm (in the ^1H NMR spectra) and δ = 128.0 ppm (in the ^{13}C NMR spectra), with a positive sign indicating a downfield shift. Legend: s = singlet, d = doublet, t = triplet, q = quartet, v = very, br = broad. [b] Shifts relative to external Me_4Si. [c] Shifts relative to external $BF_3{\cdot}OEt_2$. [d] Since relaxation of carbon or lithium without H is much slower than that of a CH or $(\mu\text{-H})_2Li$ unit, the relative areas of cage carbons or *endo*-cage lithium could not be measured accurately. [e] Shifts relative to external aqueous $LiNO_3$.

resonances of the monosodium species **I** and **II** are in the region of –0.25 to –0.69 ppm; these resonances are basically unchanged from those of their nido precursors.[16] In contrast to **I** and **II**, the apical B–H resonances of the other compounds are shifted downfield to the –1.49 to –2.02 ppm range. Since other monosodium compounds are also included in this latter group, it is not possible to assess the significance of these downfield shifts.

The ^{11}B NMR spectra of **III**, **IV**, and **VIII**, a monosodium, a mixed sodium lithium, and a dilithium deriv-

Table V. Infrared Absorptions (cm^{-1}; C_6D_6 vs C_6D_6)[a]

compd	absorption
I	3098 (s, s), 3080 (m, s), 3020 (w, s), 2950 (s, s), 2900 (sh), 2840 (sh) [ν(C–H)], 2536 (vs), 2464 (vs) [ν(B–H)], 1820 (m) [B–H–B(bridge)], 1480 (m), 1410 (sh) [(CH)asym], 1348 (ws), 1320 (w, br), 1280 (s) [(CH)sym], 1150 (w, br), 990 (s, br), 831 (vvs, br) [(CH)], 775 (m, s), 680 (s, br), 620 (m, s)[ν(Si–C)], 480 (vw, s), 389 (m, s)
II	3185 (m, s), 3110 (sh), 2954 (s, br), 2896 (s, br), 2863 (s, br) [ν(C–H)], 2707 (sh), 2524 (s, br), 2420 (s, br) [ν(B–H)], 2273 (s, br), 2260 (sh), 2234 (m, br), 1970 (m, br) [B–H–B(bridge)], 1453 (s, s) [(CH)asym], 1248 (s, vs) [(CH)sym], 1042 (s, s), 1028 (sh), 844 (s, s), 753 (s, s)
III	3160 (s, s), 2940 (vs, vbr), 2890 (sh) [ν(CH)], 2490 (vs, vbr), 2420 (sh) [ν(BH)], 2295 (s, s), 2250 (s, s), 2200 (sh), 2140 (sh), 1960 (w, w) [B–H–B(bridge)], 1400 (m, vbr) [(CH)asym], 1300 (m, s), 1270 (sh), 1240 (m, s) [(CH)sym], 1160 (w, br), 1120 (w, w), 1030 (m, w), 970 (m, s), 920 (m, s), 850 (m, vbr), [(CH)], 750 (s, s), 730 (sh), 680 (s, s), 660 (sh), 620 (s, s) [ν(Si–C)], 560 (w, s), 520 (m, s), 400 (sh), 380 (vs, br), 270 (w, br)
IV	2980 (s, s), 2920 (m, s), 2905 (sh), 2880 (vw, s), 2840 (sh), 2820 (sh) [ν(C–H)], 2520 (s, br), 2450 (s, br) [ν(B–H)], 2290 (s, br), 2160 (m, br), 2140 (m, br), 2030 (vw, s), 1640 (vw, br), 1550 (sh), 1520 (sh), 1510 (s, br), 1490 (sh), 1420 (m, br), 1380 (sh), 1360 (sh) [(CH)asym], 1210 (s, br), 1170 (w, br) [(CH)sym], 1080 (vw, br), 890 (sh), 870 (sh), 850 (sh), 840 (vvs, br), 770 (s, s), 690 (s, s), 680 (sh), 640 (s, s), 630 (sh) [ν(Si–C)]
V	3515 (s, s), 3440 (m, br), 3250 (s, s), 3190 (sh), 2960 (sh), 2880 (vs, vbr) [ν(C–H)], 2730 (m, s), 2700 (m, s), 2650 (s, s), 2600 (sh), 2490 (vs, vbr), 2420 (s, br) [ν(B–H)], 2360 (sh), 2300 (s, s), 2260 (s, vs), 2200 (sh), 2140 (vs, vbr), 1940 (m, br), 1890 (sh), 1850 (sh), 1610 (sh), 1350 (sh) [(CH)asym], 1230 (vs, vbr), [(CH)sym]
VI	3530 (w, s), 3360 (w), 2930 (m, s), 2890 (sh), 2860 (sh) [ν(C–H)], 2500 (s, s), 2430 (s, s) [ν(B–H)], 2260 (s, s), 2140 (vs, s), 1300 (w) [(CH)asym], 1240 (w, s) [(CH)sym], 1165 (w, br), 1110 (w, s), 1030 (w, br), 970 (w, br), 915 (w, s), 830 (m, s) [(CH)], 680 (m, s), 630 (sh) [ν(Si–C)], 520 (w, br), 370 (w, s)
VII	2980 (vs, s), 2930 (sh), 2940 (sh), 2935 (vw, s), 2925 (m, s), 2915 (sh), 2900 (sh), 2870 (vw, s), 2880 (vw, s) [ν(C–H)], 2548 (m, s), 2509 (m, s), 2469 (sh), 2460 (sh) [ν(B–H)], 3212 (vs, s), 2280 (s, s), 2160 (s, s), 2140 (sh), 1680 (vw, s), 1670 (vw, s), 1515 (s, br), 1425 (w, br), 1370 (w, s)[(CH)asym], 1270 (sh), 1260 (vs, s), 1250 (sh), 1210 (w, br) [(CH)sym], 1116 (vw), 990 (w, br), 860 (sh), 850 (vvs, br), 770 (m, br), 690 (w, br), 630 (m, s) [ν(Si–C)]
VIII	3721 (vw, s), 3528 (m, s), 3457 (m, br), 3391 (m, s), 3125 (w, s), 2954 (vs, s), 2899 (sh), 2859 (sh) [ν(C–H)], 2508 (vs, s), 2421 (vs, s) [ν(B–H)], 2285 (s, br), 2220 (m, s), 2137 (vs, s), 1599 (m, br), 1504 (vs, br), 1392 (s, s)[(CH)asym], 1243 (s, s), 1137 (s, br) [(CH)sym], 973 (m, s), 939 (m, s), 890 (sh), 870 (s, s), 820 (m, s), 755 (m, s), 655 (m, s), 592 (m, s), 560 (sh), 513 (w, br)
IX	3530 (s, s), 3440 (m, br), 3370 (m, br), 3200 (sh), 3130 (m, s), 2960 (m, s), 2870 (sh), 2840 (s, br), 2810 (sh)[ν(C–H)], 2690 (w, br), 2650 (w, br), 2590 (sh), 2510 (vs, vbr), 2480 (sh), 2380 (m, br) [ν(B–H)], 2270 (m, s), 2210 (w, s), 2135 (vs, vbr), 2050 (sh), 1570 (w, br), 1525 (sh), 1510 (sh), 1495 (sh), 1480 (sh) [(CH)asym], 1290 (w, br), 1260 (sh), 1245 (m, br), 1210 (m, br), 1180 (m, br) [(CH)sym]
X	3104 (w, s), 3024 (w, s), 2913 (sh), 2824 (sh) [ν(C–H)], 2689 (m, s), 2640 (m, s), 2591 (s), 2425 (s) [ν(B–H)], 1978.8 (m) [B–H–B(bridge)], 1616.7 (m, s), 1450 (m, s), 1415 (sh) [(CH)asym], 1358 (ws), 1328.8 (s, s), 1292 (s) [(CH)sym], 1158.1 (w, br), 977 (w, br), 845.8 (vvs, br) [(CH)], 703 (m, s), 634 (m, s) [ν(Si–C)], 520.7 (m, s), 504.5 (m, s)
XI	2965 (sh), 2880 (vs, vbr) [ν(C–H)], 2720 (m, s), 2690 (m, s), 2645 (s, s), 2605 (sh), 2495 (vs, vbr), 2418 (s, br) [ν(B–H)], 2367 (sh), 2300 (s, s), 2250 (s, vs), 2195 (sh), 2120 (vs, vbr), 1943 (m, br), 1895 (sh), 1850 (sh), 1620 (sh), 1360 (sh) [(CH)asym], 1235 (vs, vbr) [(CH)sym]
XII	2931 (s, s), 2860.5 (m, s), 2825.2 (m, s), 2790 (m, s), [ν(C–H)], 2484.4 (sh), 2425.6 (m, br), 2355.1 (m, br) [ν(B–H)], 2308.1 (m, s), 2261.1 (m, s), 1460.7 (sh) [(CH)asym], 1343.2 (w, s), 1290.3 (w, br), 1237.4 (m, br), 1031.7 (s, s), 943.6 (m, s), 843.7 (w, br), 673.3 (m, w)
XIII	2961 (s), 2900 (m) [ν(CH)], 2588 (vs) [ν(BH)], 1949 (w), 1884 (w), 1712 (mw), 1518 (mw), 1456 (br, sh), 1410 (m)[δ(CH)asym], 1335 (mw), 1269 (sh), 1252 (vs), 1246 (ms) [δ(CH)sym], 1144 (mw), 1121 (m), 1100 (mw), 1060 (m), 1048 (ms), 986 (mw), 974 (m), 962 (s), 935 (w), 840 (vvs) [ρ(CH)], 791 (m), 625 (s)
XIV	2960 (vs, s), 2900 (sh, w), [ν(CH)], 2600 (vs, s), 2330 (mw) [ν(BH)], 1945 (br), 1715 (w, br), 1445 (w), 1420 (w) [δ(CH)asym], 1330 (w), 1255 (vs, s), 1230 (ms) [δ(CH)sym], 1150 (w), 1080 (w), 989 (w), 840 (vs, s) [ρ(CH)], 795 (sh), 625 (ms), 600 (sh)
XV	2950 (m) [ν(CH)], 2600 (vs), 2400 (m) [ν(BH)], 2250 (m), 2000 (w), 1520 (w), 1470 (w), 1420 (w) [δ(CH)asym], 1250 (m), 1210 (s) [δ(CH)sym], 1100 (m), 1060 (m), 985 (m), 900 (s), 840 (s) [ρ(CH)], 660 (m)

[a] Legend: v = very, s = strong or sharp, m = medium, w = weak, sh = shoulder, br = broad.

ative, are shown in Figure 2. All show the same general pattern, that is, an apical boron resonance, with a relative intensity of 1, around −50 ppm with the three basal borons having resonances in the −4 to +21 ppm region. Depending on the complex, the ratios of the intensities of the basal boron resonances are in a 1:1:1 or 2:1 pattern. However, information about the nature of the metal–carborane interactions can be obtained from the apical boron resonances. Table IV shows that apical boron resonances are all in the −45 to −53 ppm range and are essentially the same as those found for the respective nido precursors (−49.3 to −51.8 ppm).[16] This is in sharp contrast to the situation found when other main-group metals, such as tin,[6,27] or transition metals[24] coordinate with the carborane to form metallacarboranes. In these cases coordination gives rise to large downfield shifts of about 45 ppm (in the case of tin, from −50 to −4.7 ppm). These shifts have been rationalized in terms of removal of carborane electron density through metal bonding.[27] The apical boron and the capping metal compete directly for electron density in the C_2B_3 carborane ring, and any covalent interactions between the metal and the carborane ligand should deshield the apical boron by drawing electron density away from it. The fact that the capping group 1 metals in **I–XII** do not materially perturb the electron density on the apical boron, at least as seen by ^{11}B NMR, is a strong indication that the interaction between the capping metal and the carborane is mainly electrostatic in nature with little charge transfer to the metal. Mulliken charge distributions obtained from MNDO–SCF calculations on the model compound **XVI** gave a charge of −0.267 on the apical boron, compared to Mulliken charge of −0.256, −0.342, and −0.056 calculated for the apical borons of its neutral nido precursor, dianion, and tin complex.[28]

The proton-decoupled ^7Li NMR spectra of **V** and **XII** show broad resonances at −1.82 and −1.60 ppm, respectively. These resonances relax very fast on an NMR time scale and are near the standard chemical shift value of 0 ppm of the purely ionic $LiNO_3$. Therefore, they can be assigned to the exo-polyhedral Li metal. The dilithium species **XII** also shows an additional ^7Li NMR resonance of −6.08 ppm, indicating the presence of two different

(27) Maguire, J. A.; Fagner, J. S.; Siriwardane, U.; Banewicz, J. J.; Hosmane, N. S. *Struct. Chem.* **1990**, *1*, 583.

(28) Maguire, J. A.; Ford, G. P.; Hosmane, N. S. *Inorg. Chem.* **1988**, *27*, 3354.

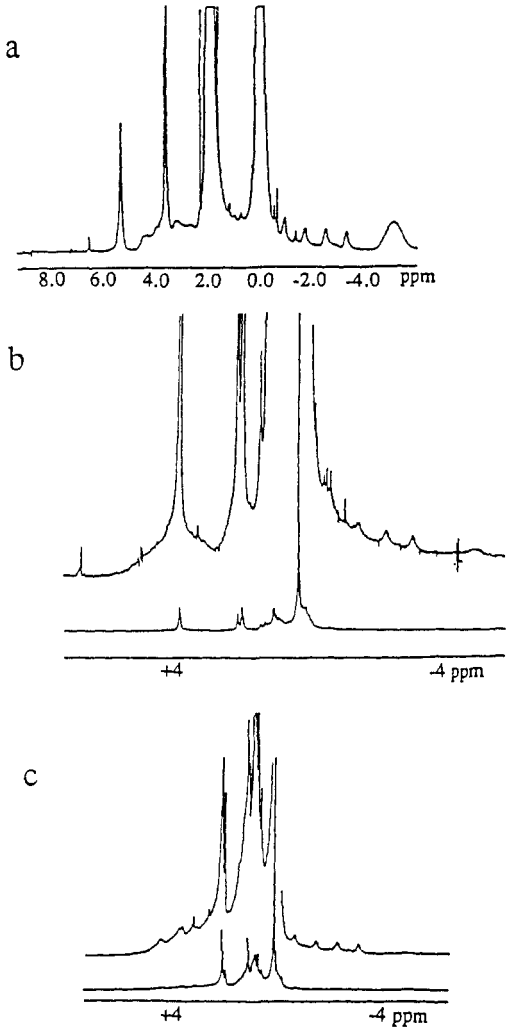

Figure 1. ^{1}H NMR spectra of (a) *nido*-1-Na(C_4H_8O)-2-($SiMe_3$)-3-(H)-2,3-$C_2B_4H_5$ (**III**), (b) *closo-exo*-Li(C_4H_8O)-1-Na(C_4H_8O)-2,3-($SiMe_3$)$_2$-2,3-$C_2B_4H_4$ (**IV**), and (c) unsolvated *closo-exo*-Li-1-Li-2-($SiMe_3$)-3-(Me)-2,3-$C_2B_4H_4$ (**VIII**).

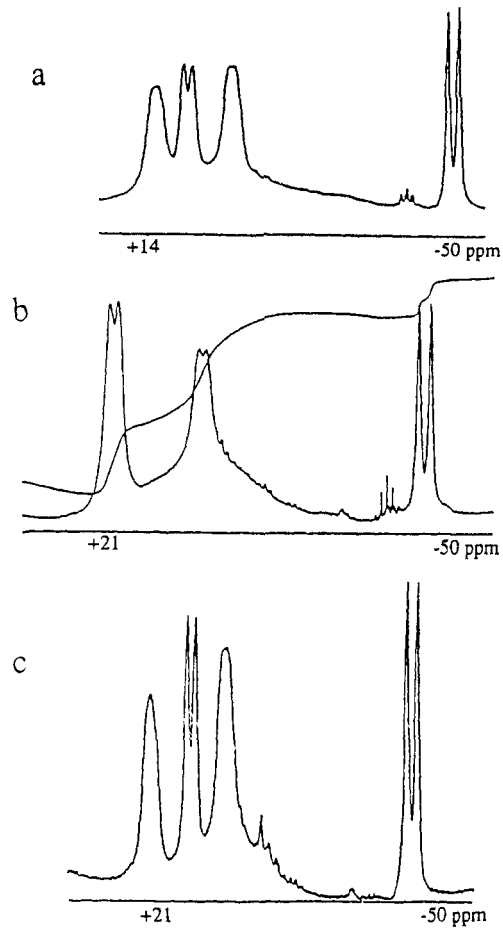

Figure 2. ^{11}B NMR spectra of the representative Na-, NaLi-, and Li_2-incorporated carborane compounds: (a) *nido*-1-Na(C_4H_8O)-2-($SiMe_3$)-3-(H)-2,3-$C_2B_4H_5$ (**III**), (b) *closo-exo*-Li(C_4H_8O)-1-Na(C_4H_8O)-2,3-($SiMe_3$)$_2$-2,3-$C_2B_4H_4$ (**IV**), and (c) unsolvated *closo-exo*-Li-1-Li-2-($SiMe_3$)-3-(Me)-2,3-$C_2B_4H_4$ (**VIII**).

bonding environments of the Li metals *in* **XII**. The chemical shift of the second, upfield resonance in **XII** is similar to those found in the ^{7}Li NMR spectra of lithium compounds with aromatic anions[29] and can be assigned to the apical Li metal in **XII**. The increased broadness in the ^{1}H-coupled ^{7}Li NMR spectra could be due to the presence of Li–H–B bridges as found in the crystal structure of **XII**. It should be pointed out that the properties and structures of these organolithium π complexes, including cyclopentadienyllithium, have been shown to arise from predominantly ionic interactions between the lithium and the particular carbanion, with covalent bonding making, at best, minor contributions.[30,31] The NMR data listed in Table IV were obtained in benzene; ^{7}Li NMR data were also collected on **XII** in TMEDA and THF. In TMEDA solvent, two ^{7}Li NMR resonances were observed for **XII**, one at $\delta = -0.60$ ppm and another at $\delta = -5.58$ ppm; these can be identified as the respective solvent shifted exo-polyhedral and endo-polyhedral ^{7}Li resonances. Rapid decomposition of **VII** in THF prevented the attainment of a reliable ^{7}Li NMR spectrum. Therefore, it seems that even in the more coordinating solvents, such as TMEDA, extensive ion pairing occurs, much like that found in the less coordinating solvents, such as benzene. In this regard, it should be noted that the dielectric constants of TMEDA and benzene are quite similar (at 25 °C, $\epsilon = 2.7$ for TMEDA and $\epsilon = 2.3$ for C_6H_6).[32] The ^{7}Li NMR of **XII** (in C_6D_6) after one Li was replaced by a $[(C_6H_5)_4P]^+$ retained only the −6.08 ppm resonance, indicating that, as expected, a metal in the exo-polyhedral position is less tightly bound than is one in the apical position. Thus, the ^{7}Li NMR spectra of both **V** and **XII** have eliminated any ambiguity that might have existed in the formulations of the mixed-metal species *closo-exo*-Li(THF or TMEDA)-1-Na(THF or TMEDA)-2-($SiMe_3$)-3-(R)-2,3-$C_2B_4H_4$ [R = $SiMe_3$ (**IV** or **XI**), Me (**V**), H (**VI**)]. It is of interest to note, that, if the above ^{7}Li NMR assignments are correct, the location of the group 1 metal seems to be more a function of the order in which the metals are introduced than of the nature of the metal. That is, the metal associated with the removal of the first bridged hydrogen will occupy the apical position, while the metal introduced later is exo-polyhedral.

Although the NMR and IR spectra of *closo*-1,2-($SiMe_3$)$_2$-1,2-$C_2B_4H_4$ (**XIII**) have been discussed elsewhere,[15] they

(29) Cox, R. H.; Terry, H. W., Jr.; Harrison, L. W. *J. Am. Chem. Soc.* **1971**, *93*, 3297.
(30) Setzer, W. N.; Schleyer, P. v. R. *Adv. Organomet. Chem.* **1985**, *24*, 353.
(31) (a) Waterman, K. C.; Streitwieser, A., Jr. *J. Am. Chem. Soc.* **1984**, *106*, 3138. (b) Streitwieser, A., Jr. *Acc. Chem. Res.* **1984**, *17*, 353.
(32) (a) For C_6H_6 and THF: Riddick, J. A.; Bunger, W. B.; Sakano, T. K. *Techniques of Chemistry: Organic Solvents Physical Properties and Methods of Purification*, 4th Ed.; John Wiley: New York, 1986; Vol. II. (b) For TMEDA: Agami, C. *Bull. Soc. Chim. Fr.* **1970**, 1619.

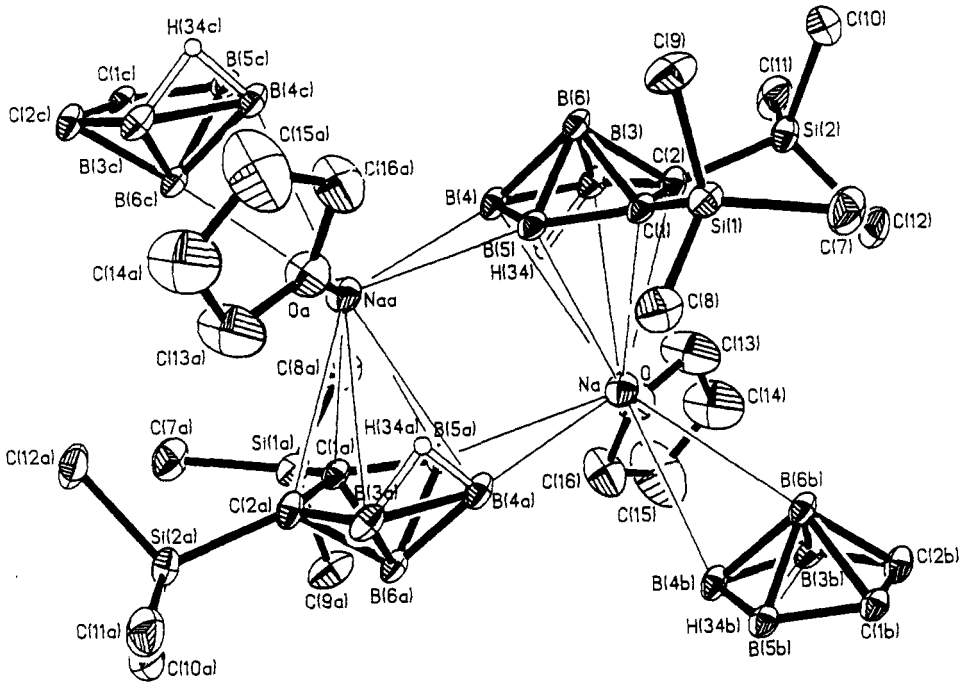

Figure 3. Perspective view of the dimeric form of *nido*-1-Na(C_4H_8O)-2,3-($SiMe_3$)$_2$-2,3-$C_2B_4H_5$ (**I**) showing the atom numbering scheme with thermal ellipsoids, drawn at the 40% probability level.

are included in Table IV in order to compare the data with those of **XIV** and **XV**. All the spectra indicate the presence of *closo*-carborane cages without the metal atoms. The presence of three doublets in a 1:1:2 ratio, in the ^{11}B NMR spectra of both **XIV** and **XV**, is consistent with the formulation (see Experimental Section and Scheme I) that the *C*-$SiMe_3$ and *C*-Me or H groups occupy adjacent vertices of an octahedron. The significant upfield shifts of the cage carbon resonances from those of the dilithium precursors, **VII–IX**, as well as the *nido*-2-($SiMe_3$)-3-(R)-2,3-$C_2B_4H_6$ (R = $SiMe_3$, Me, and H) derivatives[16] are consistent with the closo structures of **XIII–XV** which are delocalized to some degree.

The IR absorption peaks of the compounds **I–XV** in C_6D_6 are given in Table V. They all show absorptions that are consistent with the formulas given in the Experimental Section. One characteristic feature of the IR spectra of **I–XII** is that, unlike the corresponding neutral *nido*-carboranes and the group 14 metallacarboranes,[6,16] the group 1 carborane compounds show multiple peaks in the B–H stretching region of 2400–2700 cm^{-1} (see Table V). This B–H splitting is also found in the IR spectra of **XI** and **XII** in TMEDA solvent and, though somewhat attenuated, in the IR spectrum of **XII** in C_6H_6 when the two lithiums were replaced with $[EtPh_3P]^+$ cations. Nonequivalent terminal hydrogens could arise from the different ionic environments of the carborane cage hydrogens in group 1 ion clusters. The X-ray structure of **XII** (see Figure 6) shows one lithium occupying an apical position above the C_2B_3 open face of the carborane, while the other lithium is situated exo-polyhedrally and interacts strongly with two of the four terminal hydrogens. The nonequivalence of the terminal hydrogens in the nido monosodium compounds can be seen in Figures 3–5. The solubility behavior of these species and the measured molar masses of **I** and **VII**, coupled with the ^7Li NMR spectra of **V** and **XII**, discussed above, indicate that in low dielectric constant solvents such as used in this study (the highest dielectric constant solvent is THF, with $\epsilon = 7.6$ at 25 °C),[32] there is extensive ion aggregation and neutral ion clusters, whose structures are probably not too different

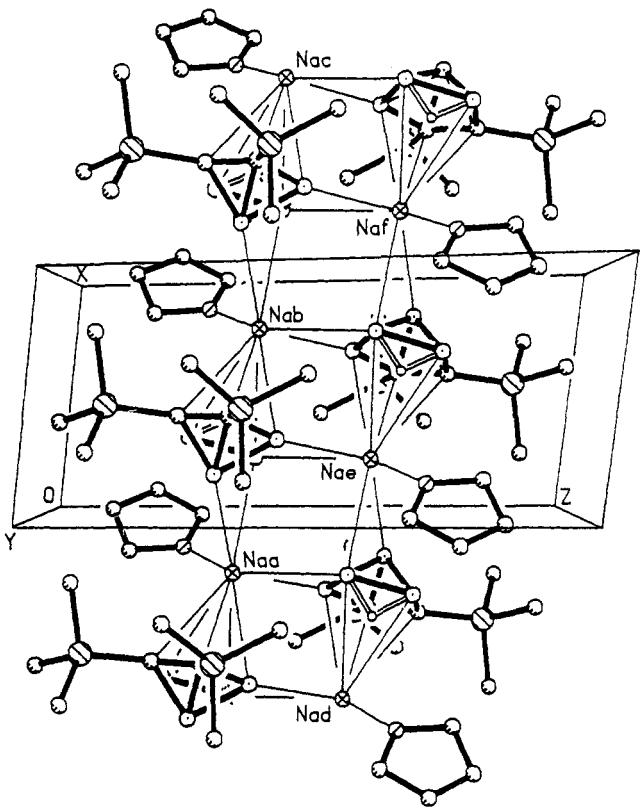

Figure 4. Packing diagram showing the extended interactions between the dimeric clusters of **I**.

from those shown in Figure 6 and in the monomer units of Figures 3 and 5, may exist in solution. In all of these, nonequivalent terminal cage hydrogens would be present. Hawthorne and co-workers[33] have recently observed splittings of the B–H stretching bands in the solid state IR spectra of some icosahedral lanthanacarboranes. They have speculated that this may be a consequence of a strongly ionic interaction between the cationic lanthanide

(33) Manning, M. J.; Knobler, C. B.; Khattar, R.; Hawthorne, M. F. *Inorg. Chem.* **1991**, *30*, 2009.

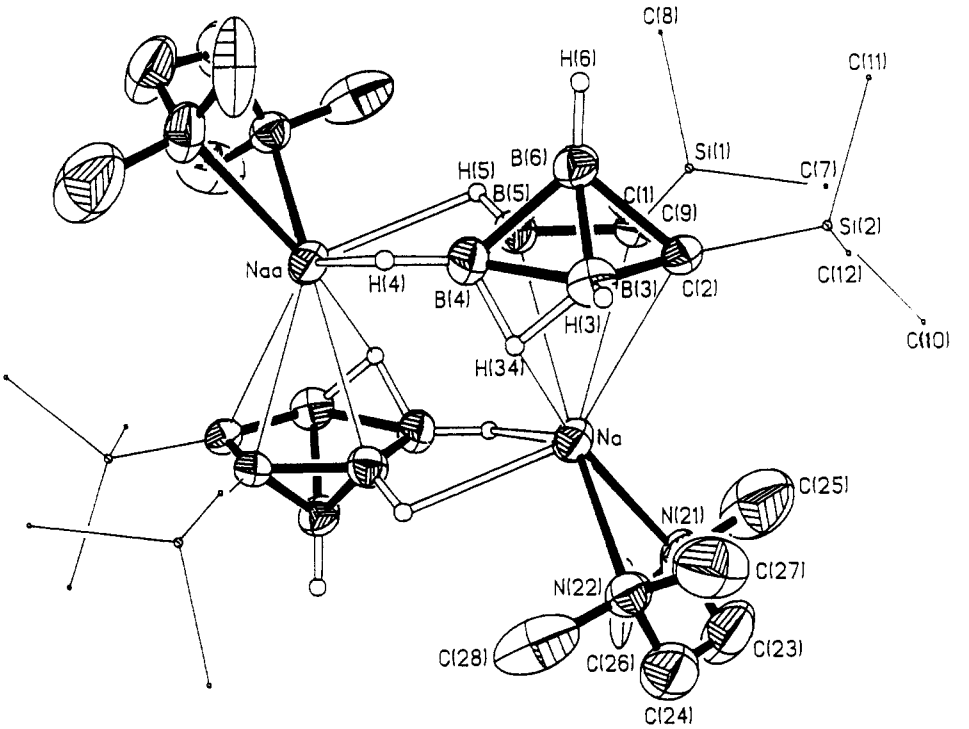

Figure 5. Perspective view of a discrete dimeric unit of *nido*-1-Na[$(Me_2NCH_2)_2$]-2,3-$(SiMe_3)_2$-2,3-$C_2B_4H_5$ (**X**) showing the atom numbering scheme with thermal ellipsoids, drawn at the 40% probability level. The atoms of the $SiMe_3$ groups are drawn with the circles of arbitrary radii and the methyl and methylene H's are omitted for clarity.

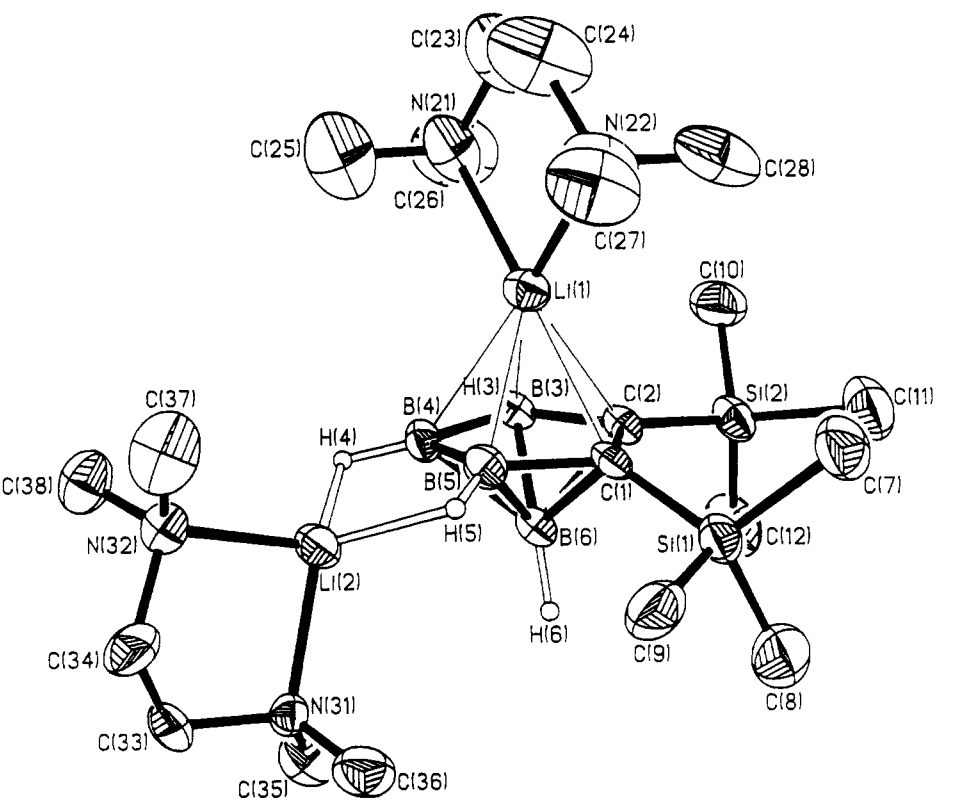

Figure 6. Perspective view of the zwitterionic *closo*-dilithiacarborane, *exo*-4,5-[$(\mu$-H)$_2$Li$(Me_2NCH_2)_2$]-1-Li[$(Me_2NCH_2)_2$]-2,3-$(SiMe_3)_2$-2,3-$C_2B_4H_4$ (**XII**) with thermal ellipsoids drawn at the 40% probability level and showing the atom numbering scheme. The atoms of the $SiMe_3$ groups are drawn with the circles of arbitrary radii and the methyl and methylene H's are omitted for clarity.

and the anionic carborane, in that the terminal hydrogens on the upper C_2B_3 ring would interact more strongly with the capping metal cation than would the more remote lower ring and apical terminal hydrogens. This could give rise to sufficiently different B–H force constants for the two groups of hydrogens so as to produce band splitting. These authors have suggested that such splitting may be diagnostic for the presence of ionic bonding in metallacarborane complexes. In addition to the B–H band splittings found in **I**–**XII**, the IR spectrum of the mixed-valence trinuclear manganacarborane {[Li(THF)][Li(TMEDA)]$_2$}{*commo*-Mn_3[2,3-$(SiMe_3)_2$-2,3-$C_2B_4H_4]_4$} also

shows splitting in the B–H stretching bands. Its X-ray structure yields bond lengths that indicate that the lithium counterions interact strongly with several of the terminal B–H hydrogens.[25b] Therefore, some caution must be exercised in using the B–H IR splitting to assess intracage bonding in anionic metallacarboranes, since interactions with the exo-polyhedral counterions, rather than the capping metal, could also produce such splittings.

Crystal Structures of the Dimeric *nido*-Natracarboranes, 1-Na(C_4H_8O)-2,3-($SiMe_3$)$_2$-2,3-$C_2B_4H_5$ (I) and 1-Na[(Me_2NCH_2)$_2$]-2,3-($SiMe_3$)$_2$-2,3-$C_2B_4H_5$ (X), and the Zwitterionic *closo*-Dilithiacarborane, *exo*-4,5-[(μ-H)$_2$Li(Me_2NCH_2)$_2$]-1-Li[(Me_2NCH_2)$_2$]-2,3-($SiMe_3$)$_2$-2,3-$C_2B_4H_4$ (XII), and Molecular Orbital Analysis. Compounds **I**, **X**, and **XII** were also characterized by single crystal X-ray diffraction. Tables I and II give the pertinent crystallographic information and atom coordinates, while selected bond distances and bond angles are listed in Table III. Preliminary structural results on **I** have been published in a previous communication.[7] The solid state structure of compound **I** was described as an extended array of tightly bound [1-Na(THF)-2,3-($SiMe_3$)$_2$-2,3-$C_2B_4H_5$]$_2$ dimers stacked on top of one another. Figure 4 shows the unit cell packing and a portion of the array, while Figure 3 gives a more detailed view of the immediate environment around the sodium ions. These figures show that the capping sodiums are not centered above the carborane faces but are dislocated away from the side of the carborane having the bridged hydrogen [the Na–C(1) and Na–B(5) bond distances are 2.832 and 2.920 Å, respectively, while the Na–C(2) and Na–B(3) distances are 3.017 and 3.302 Å, respectively (see Table III and Figure 3)]. The average distance of the capping Na in Figure 3 from its ring atoms [C(1), C(2), B(3), B(4), and B(5)] is 3.1 Å, which is about the same as that from the neighboring carborane atoms B(4a) [2.995 Å] and B(6b) [3.179 Å]. Therefore, an alternate, and perhaps better, description of the structure shown in Figure 4 is that of pairs of chains of carborane anions that are separated by [Na(THF)]$^+$ ions, which gives rise to an arrangement in which each Na^+ is surrounded by three carborane anions and a THF under the influence of electrostatic forces. Such aggregates are common for organometallic compounds of sodium.[34] When the THF is replaced by the larger TMEDA molecule, the chain structure is broken and more isolated dimers, such as those found in 1-Na(TMEDA)-2,3-($SiMe_3$)$_2$-2,3-$C_2B_4H_5$ (**X**), are formed, as shown in Figure 5. As one would expect for predominantly ionic metal–carborane interactions, the equivalent sodium–carborane atom distances in **I** and **X** are essentially the same.

The structure of the *closo*-dilithiacarborane *exo*-4,5-[(μ-H)$_2$Li(Me_2NCH_2)$_2$]-1-Li[(Me_2NCH_2)$_2$]-2,3-($SiMe_3$)$_2$-2,3-$C_2B_4H_4$ (**XII**) is shown in Figure 6, and the pertinent bond lengths and bond angles are listed in Table III. Figure 6 shows that the two lithiums occupy quite different positions relative to the carborane face, with one lithium occupying an apical position above the C_2B_3 face and the other located exo-polyhedrally and about halfway between B(4) and B(5) and directed down below the plane of the C_2B_3 face [the Li(2)–B(4) and Li(2)–B(5) bond distances are 2.226 and 2.241 Å, respectively (see Table III)]. In contrast to the structures of the sodium species shown in Figures 4 and 5, there is not extensive association between metallacarborane units. In an effort to ascertain the extent to which these lithium arrangements are dictated by interactions within the dilithiacarborane itself rather than crystal lattice forces, MNDO–SCF calculations were carried out on the model compound *closo-exo*-4,5-[(μ-H)$_2$Li(TMEDA)]-1-Li(TMEDA)-2,3-$C_2B_4H_6$ (**XVI**). MNDO has been found to be useful in rationalizing the structures of a number of organolithium salts,[30] and $[C_2B_4H_6]^{2-}$ has been shown to serve as a good model for the trimethylsilyl derivatives.[28] The MNDO optimized geometry of **XVI** possesses all the general structural characteristics of **XII**, as shown in Figure 6; the optimized geometric parameters are in reasonable agreement with those given in Tables II and III (see supplementary table S-3 for the MNDO optimized bond distances in **XVI**). Therefore, the structure shown in Figure 6 can be assumed to be a minimum energy structure arising from interactions among the carborane and its two Li(TMEDA) groups. Although crystal structures could not be obtained for the mixed sodium/lithium compounds, **IV–VI** and **XI**, the ^{7}Li NMR spectrum of **V** is consistent with a structure in which the Li is exo-polyhedral and the Na occupies the apical position (*vide supra*). At present, there is no reason to assume that such descriptions cannot be applied to the other mixed-metal species found in this study. Another aspect of the crystal structure of **XII** also tends to favor a description in which predominantly electrostatic interactions between the lithium metals and their neighboring groups dictate the structures. Molecular orbital calculations on groups 13 and 14 metallacarboranes and their Lewis base complexes have shown that the participation of a capping metal's valence p orbitals in bonding will give rise to a slip distortion of the metal and an orientation of the base over the boron side of the C_2B_3 face of the carborane, while ligand–ligand repulsion would favor the base being directly opposite the carborane cage.[11,27,28] The orientations of the TMEDA molecules in **XII**, as shown in Figure 6, seem to be governed more by electrostatic rather than metal–ligand covalent interactions. Mulliken charges on {1-Li(TMEDA)-2,3-$C_2B_4H_6$}$^-$ (**XVII**), calculated from MNDO, showed that the negative charge was distributed mainly, and fairly evenly, over the cage boron atoms [the Mulliken charges in **XVII** were −0.228, −0.222, −0.225, and −0.224 for the atoms equivalent to B(6), B(5), B(3), and B(4), respectively]. Therefore, the location of the second Li(TMEDA)$^+$ unit close to the B(4)–B(5)–B(6) plane is not unexpected. The Li(2)–H(4) and Li(2)–H(5) bond lengths of 1.93 and 1.97 Å, respectively, in **XII** are well within the sum of their van der Waals radii[35] and indicate a direct interaction between the lithium and these terminal cage hydrogens. These distances are similar to the values of 2.11 Å determined from neutron and X-ray diffraction studies for the dibridged Li–H distances in $LiB(CH_3)_4$.[36] Although it is an open question as to how much, if any, such bridging interactions stabilize **XII** and, presumably, **IV–IX** and **XI**, they do provide an explanation for the splitting found in the B–H IR stretching bands of these compounds (*vide supra*).

The solution spectra of the group 1 C_2B_4 carboranes can be accounted for by assuming that they exist in solution as tightly bound ion pairs or ion clusters, similar to the solid state structures shown in Figures 5 and 6. The failure of strong heterogeneous bases, such as NaH, to deprotonate the monosodium complexed C_2B_4 carboranes while easily reacting with the monosodium compound of the larger

(34) Schade, C.; Schleyer, P. v. R. *Adv. Organomet. Chem.* **1987**, *27*, 169.

(35) Bondi, A. *J. Phys. Chem.* **1964**, *68*, 441.

(36) Rhine, W. E.; Stucky, G.; Peterson, S. W. *J. Am. Chem. Soc.* **1975**, *97*, 6401.

cage C_2B_9 carboranes can also be rationalized on the basis of the former being weaker acids and better ion pair formers than their larger cage analogues. From the MNDO calculated heats of formation of the species involved, ΔH for eq 1 is determined to be −56 kcal/mol. Although this

$$C_2B_9H_{12}^- + C_2B_4H_6^{2-} \rightarrow C_2B_9H_{11}^{2-} + C_2B_4H_7^- \quad (1)$$

is an estimate for the isolated ion reaction in the gas phase, it does indicate that $C_2B_4H_7^-$ is less acidic than $C_2B_9H_{12}^-$. Mulliken charge distributions show that the negative charge on the smaller anion is more localized than on the larger one; therefore, the former should form the stronger ion pair. Grimes and co-workers[37] have studied the kinetics of the deprotonation reactions of *nido*-2,3-$RR'C_2B_4H_6$ (where R = alkyl, arylmethyl, and phenyl; R′ = R, H) with NaH or KH in THF. Their results showed a decrease in the rate as the sizes of R and R′ increased and all data were consistent with deprotonation occurring at the surface of the metal hydride through the direct reaction of a bridged carborane hydrogen with a H^- ion in the hydride lattice. For an ion pair in which $Na(THF)^+$ or $Na(TMEDA)^+$ occupies an apical position similar to those shown in Figures 3–5, the bridged hydrogen would be effectively buffered by the capping solvated metal ion and the terminal carborane hydrogens, thus blocking it from direct reaction with a hydride lattice site. On the other hand, soluble reactants, such as the *t*-BuLi or metal halides, would not be as subject to such a blockage and could react with the ion pair to form the mixed sodium lithium or other metallacarboranes.

(37) Fessler, M. E.; Whelan, T.; Spencer, J. T.; Grimes, R. N. *J. Am. Chem. Soc.* **1987**, *109*, 7416.

Acknowledgment. This work was supported by grants from the National Science Foundation (CHE-9100048), the Robert A. Welch Foundation (N-1016), and the donors of the Petroleum Research Fund, administered by the American Chemical Society.

Supplementary Material Available: Tables of anisotropic displacement parameters for **I**, **X**, and **XII** (Table S-1), H atom coordinates and isotropic displacement coefficients for **I**, **X**, and **XII** (Table S-2), and selected bond lengths for **XVI** calculated by MNDO (Table S-3) (6 pages). Ordering information is given on any current masthead page.

OM930051N